

8-2019

ROLE OF c-MET and EGFR IN ACQUIRED RESISTANCE TO PARP INHIBITORS IN TRIPLE-NEGATIVE BREAST CANCER

Clinton Yam

Follow this and additional works at: https://digitalcommons.library.tmc.edu/utgsbs_dissertations



Part of the [Biology Commons](#), and the [Medicine and Health Sciences Commons](#)

Recommended Citation

Yam, Clinton, "ROLE OF c-MET and EGFR IN ACQUIRED RESISTANCE TO PARP INHIBITORS IN TRIPLE-NEGATIVE BREAST CANCER" (2019). *The University of Texas MD Anderson Cancer Center UTHealth Graduate School of Biomedical Sciences Dissertations and Theses (Open Access)*. 952.
https://digitalcommons.library.tmc.edu/utgsbs_dissertations/952

This Thesis (MS) is brought to you for free and open access by the The University of Texas MD Anderson Cancer Center UTHealth Graduate School of Biomedical Sciences at DigitalCommons@TMC. It has been accepted for inclusion in The University of Texas MD Anderson Cancer Center UTHealth Graduate School of Biomedical Sciences Dissertations and Theses (Open Access) by an authorized administrator of DigitalCommons@TMC. For more information, please contact digitalcommons@library.tmc.edu.

ROLE OF c-MET and EGFR IN ACQUIRED RESISTANCE TO PARP INHIBITORS
IN TRIPLE-NEGATIVE BREAST CANCER

by

Clinton Yam, MD

APPROVED:

Jeffrey Chang, Ph.D.
Advisory Professor

Mien-Chie Hung, Ph.D.

Bin Wang, Ph.D.

Jennifer Litton, M.D.

Stacy Moulder, M.D., M.S.

APPROVED:

Dean, The University of Texas
MD Anderson Cancer Center UTHHealth Graduate School of Biomedical Sciences

ROLE OF c-MET AND EGFR IN ACQUIRED RESISTANCE TO PARP
INHIBITORS IN TRIPLE-NEGATIVE BREAST CANCER

A
THESIS

Presented to the Faculty of

The University of Texas
MD Anderson Cancer Center UTHealth
Graduate School of Biomedical Sciences

in Partial Fulfillment
of the Requirements
for the Degree of
MASTER OF SCIENCE

by
Clinton Yam, M.D.
Houston, Texas
August, 2019

Dedication

This thesis is dedicated to my family, friends, and everyone I have ever loved

ROLE OF c-MET AND EGFR IN ACQUIRED RESISTANCE TO PARP
INHIBITORS IN TRIPLE-NEGATIVE BREAST CANCER

Clinton Yam, M.D.

Advisory Professor: Jeffrey Chang, Ph.D.

Triple-negative breast cancer is associated with a poor prognosis and treatment options are limited. The Poly (ADP-ribose) polymerase (PARP) inhibitors, olaparib and talazoparib, were recently approved for metastatic breast cancer (including triple-negative breast cancer) in patients with a germline *BRCA1/2* mutation. Despite impressive response rates of ~60%, the prolongation in median progression-free survival with PARP inhibitors is modest, suggesting the emergence of resistance. We previously demonstrated that c-MET contributes to intrinsic resistance to PARP inhibitors in triple-negative breast cancer. However, whether c-MET plays a role in acquired resistance to PARP inhibitors in triple-negative breast cancer remains unclear. Here, we show that phospho-c-MET expression is higher in PARP inhibitor-resistant triple-negative breast cancer cells and the combination of talazoparib and crizotinib (multi-kinase inhibitor that inhibits c-MET) results in synergistic inhibition of cellular proliferation in PARP inhibitor-resistant cells. However, depleting c-MET in PARP inhibitor resistant cells had limited effect on talazoparib sensitivity. Notably, we found that c-MET interacts with the epidermal growth factor receptor (EGFR) in PARP inhibitor-resistant triple-negative breast cancer cells, potentially explaining the limited effect of c-MET depletion alone on talazoparib sensitivity. Together, these data suggest that the combination of c-MET, EGFR and PARP inhibition should be explored in future studies.

TABLE OF CONTENTS

| Section | Page |
|----------------------------------|-------------|
| Approval Page | i |
| Title Page | ii |
| Dedication | iii |
| Abstract | iv |
| Table of Contents | v |
| List of Illustrations | vi |
| List of Tables | vii |
| Chapter 1: Introduction | 1 |
| Chapter 2: Materials and Methods | 5 |
| Chapter 3: Results | 8 |
| Chapter 4: Discussion | 59 |
| Bibliography | 63 |
| Vita | 72 |

LIST OF ILLUSTRATIONS

| Figure Number | Title | Page |
|----------------------|--|-------------|
| Figure 1 | The PARP inhibitor-resistant triple-negative breast cancer cell lines B3 and C12 have higher levels of phospho-c-MET expression relative to the PARP inhibitor-sensitive parental triple-negative breast cancer cell line, SUM149 (parental). | 9 |
| Figure 2 | The combination of crizotinib and talazoparib results in synergistic inhibition of cellular proliferation in PARP inhibitor-resistant triple-negative breast cancer cell lines, B3 and C12. | 15 |
| Figure 3 | PARP inhibitor-resistant triple-negative breast cancer cell lines were infected with lentiviral particles carrying non-specific or c-MET targeting short hairpin RNA (shRNA) sequences. | 17 |
| Figure 4 | Following lentiviral delivery of two independent short hairpin RNAs targeting c-MET to PARP inhibitor-resistant triple-negative breast cancer cell lines, B3 and C12, expression levels of c-MET was reduced by at least 50% relative to cells receiving non-specific short hairpin RNA sequences. | 19 |
| Figure 5 | Depleting c-MET results in a modest increase in sensitivity to talazoparib in the PARP inhibitor-resistant triple-negative breast cancer cell line C12. | 21 |
| Figure 6 | Depleting c-MET in the PARP inhibitor resistant triple-negative breast cancer cell line B3 does not consistently increase sensitivity to talazoparib. | 23 |
| Figure 7 | Enhanced interaction between c-MET and EGFR but not ErbB2 is detected in the PARP inhibitor-resistant triple-negative breast cancer cell line, C12, relative to PARP inhibitor-sensitive parental (PT) triple-negative breast cancer cell line (SUM149), following treatment with talazoparib. | 27 |
| Figure 8 | Interaction between c-MET and ALK or EphA2 was not enhanced in the PARP inhibitor-resistant triple-negative breast cancer cell, C12, relative to PARP inhibitor-sensitive parental (PT) triple-negative breast cancer cells (SUM149) , following treatment with talazoparib. | 29 |
| Figure 9 | The interaction between c-MET and EGFR is enhanced in PARP inhibitor-resistant triple-negative breast cancer cells (B3 and C12) relative to PARP inhibitor-sensitive parental (PT) triple-negative breast cancer cells (SUM149), under basal conditions as well as following treatment with talazoparib. | 31 |
| Figure 10 | The PARP inhibitor-resistant triple-negative breast cancer cell lines B3 and C12 have higher levels of phospho- and total-EGFR expression relative to the PARP inhibitor-sensitive parental triple-negative breast cancer cell line, SUM149. | 33 |
| Figure 11 | Study schema for NCT02282345 | 37 |

| | | |
|-----------|--|----|
| Figure 12 | MET protein expression increased in patients with talazoparib-resistant breast cancer following treatment with single-agent talazoparib in the neoadjuvant setting. | 39 |
| Figure 13 | Patients with talazoparib-resistant breast cancer had an increase in EGFR expression following treatment with single-agent talazoparib in the neoadjuvant setting. | 41 |
| Figure 14 | Phospho-EGFR expression levels increased in patients with talazoparib-resistant breast cancer following treatment with single-agent talazoparib in the neoadjuvant setting. | 43 |
| Figure 15 | Patients with talazoparib-sensitive and talazoparib-resistant disease appeared to have similar MET copy number at baseline. Treatment with talazoparib increased MET gene copy number, with the greatest increase observed in patients with talazoparib-resistant disease. | 45 |
| Figure 16 | Patients with talazoparib-sensitive disease had higher EGFR copy number at baseline. Treatment with talazoparib increased EGFR gene copy number, with the greatest increase observed in patients with talazoparib-resistant disease. | 47 |
| Figure 17 | p-Y907 PARP1 expression is increased in resistant cell C12 but not B3, following treatment with PARP inhibitors. | 50 |
| Figure 18 | Systematic search of a public database (BioGRID) revealed 91 c-MET interacting and 1254 EGFR-interacting proteins. Of these, 33 were identified to interact with both c-MET and EGFR. | 53 |

LIST OF TABLES

| Table Number | Title | Page |
|---------------------|---|-------------|
| Table 1 | Concentrations of crizotinib and talazoparib used in the determination of the combination index for the PARP inhibitor-resistant triple-negative breast cancer cell lines B3 and C12. | 13 |
| Table 2 | List of proteins known to interact with both c-MET and EGFR | 55 |
| Table 3 | List of proteins known to interact with both c-MET and EGFR that are involved in DNA damage repair. | 57 |

CHAPTER 1. INTRODUCTION

1.1 Triple-negative breast cancer

Triple-negative breast cancers are defined by the lack of expression of three major actionable targets in breast cancer, namely, the estrogen receptor (ER), the progesterone receptor (PR), and the human epidermal growth factor receptor 2 (HER2) (1). Together, this subtype of breast cancer makes up 10-20% of primary breast cancers (2-5). In contrast with hormone receptor-positive and/or HER2-positive breast cancers, triple-negative breast cancers tend to be larger, more likely node-positive and of higher grade (6). Although triple-negative breast cancers are more likely to respond to cytotoxic chemotherapy in the neoadjuvant setting compared to other breast cancer subtypes, chemotherapy-resistant triple-negative breast cancer carries a dismal prognosis with a 40-80% risk of disease recurrence in the first 2-3 years following definitive surgical intervention (6-9).

1.2 Triple-negative breast cancer and the DNA damage response pathway

Seventy-one percent of breast cancers diagnosed in *BRCA1* mutation carriers and 25% of breast cancers diagnosed in *BRCA2* mutation carriers are triple-negative breast cancers. In contrast, only 17% of breast cancers diagnosed in non-*BRCA1/2* mutation carriers were triple-negative breast cancers (10). On average, 35% of patients with triple-negative breast cancer carry a germline *BRCA1* mutation and 8% of patients with triple-negative breast cancer carry a *BRCA2* mutation. *BRCA1/2* mutations result in defective homologous recombination, leading to accumulation of DNA damage (11), increasing the sensitivity of such tumors to DNA damaging agents such as platinum agents and poly-ADP-ribose polymerase (PARP) inhibitors (12). In addition, some *BRCA1/2*-wild type triple-negative breast cancers have defective

homologous recombination and share the increased sensitivity to DNA damaging agents observed in *BRCA1/2* mutant tumors, a phenotype commonly termed, *BRCAness* (12).

1.3 Targeted therapy in triple-negative breast cancer

Cytotoxic chemotherapy remained the only FDA-approved treatment for triple-negative breast cancer up until recently, when two randomized phase III clinical trials (13, 14) led to the approval of olaparib and talazoparib for patients with metastatic or advanced, HER2-negative breast cancer with a germline *BRCA1/2* mutation, including those with triple-negative breast cancer. The overall response rate to olaparib in the phase III OlympiAD trial in patients with measurable disease was 59.9%, compared to 28.8% in patients receiving standard therapy (13). Median progression-free survival in patients receiving olaparib was 7.0 months, versus 4.2 months in patients receiving standard therapy (13). In the phase III EMBRACA study, the response rate to talazoparib was 62.6%, compared to 27.2% in patients receiving standard therapy (14). The median progression-free survival was 8.6 months in patients receiving talazoparib and 5.6 months in patients receiving standard therapy (14). Thus, although response rates to PARP inhibitors in advanced or metastatic breast cancer are impressive, the 3-month improvement in progression-free survival is modest, suggesting the emergence of resistance to these novel agents.

1.4 Mechanisms of resistance to PARP inhibitors

Several described mechanisms of resistance to PARP inhibitors have contributed to the current paradigm. First, restoration of homologous recombination through reversion mutations in *BRCA1/2* (15) as well as concurrent mutations in *TP53BP1* (16) or *PTEN* (17) have been shown to contribute to PARP inhibitor resistance. Second, increased reliance on alternate means of DNA repair like non homologous end joining can limit the therapeutic efficacy of

PARP inhibitors (18). Third, since PARP inhibitors suppress DNA repair at replication forks and promote formation of double strand breaks (19, 20), stabilization of the replication fork can antagonize the anti-tumor effects of PARP inhibitors (21-23). Fourth, reduced PARP expression (24) or binding (25) has been shown to result in PARP inhibitor resistance as did increased expression of PARP inhibitor efflux pumps (26). Fifth, cell cycle checkpoint activation has been reported to result in cell cycle delay, giving the cancer cell time to repair damaged DNA (27), resulting in resistance to PARP inhibition. Notably, inhibition of cyclin-dependent kinase 12 (CDK12) was found to enhance sensitivity to PARP inhibitors (28-31). Additionally, increased WEE1 expression, which promotes cell cycle arrest and DNA repair, was found to result in PARP inhibitor resistance (32). Similarly, CHK1 has been shown to induce cell cycle arrest in response to DNA damage (33) and CHK1 inhibition has been shown to potentiate the effects of PARP inhibitors (34).

1.5 Receptor tyrosine kinases in PARP inhibitor resistance

In addition to the above described mechanisms of resistance to PARP inhibitors, the receptor tyrosine kinase c-MET has been shown to interact with and phosphorylate PARP1 at the Tyr907 residue, increasing its enzymatic activity and decreasing its binding to PARP inhibitors (35). Notably, in a model of intrinsic resistance to PARP inhibitors, the combination of a c-MET inhibitor and PARP inhibitor was shown to reduce proliferation of triple-negative breast cancer in vitro and in vivo (35). Interestingly, the epidermal growth factor receptor (EGFR), another receptor tyrosine kinase, has also been shown to interact with c-MET, leading to phosphorylation of PARP1 at the Tyr907 residue, contributing to PARP inhibitor-resistance in hepatocellular carcinoma (36). In triple-negative breast cancer, dual targeting of MET and EGFR was shown to inhibit tumor growth in a more consistent manner compared to inhibiting

either target alone (37) but the impact of c-MET and EGFR crosstalk signaling on PARP inhibitor resistance in triple-negative breast cancer remains unknown.

1.5 Acquired resistance to PARP inhibitors and receptor tyrosine kinases

While c-MET activity has been shown to enhance intrinsic resistance to PARP inhibitors in *BRCA1/2* wild type triple-negative breast cancer (35), its role in acquired resistance to PARP inhibitors in *BRCA1/2* deficient triple-negative breast cancer remains unclear. In addition, since coexpression of receptor tyrosine kinases has been shown to contribute to therapeutic resistance (37), significant involvement of other receptor tyrosine kinases in the setting of acquired resistance to PARP inhibitors remains a distinct possibility and an open question.

CHAPTER 2. MATERIALS AND METHODS

2.1 Cell Culture

The SUM149 cell line was obtained from Asterand Biosciences (Detroit, MI) and maintained in F12K medium containing 5% FBS, 10 mM HEPES, 1mg/ml hydrocortisone, 5 μ g/ml insulin, 100 units/ml penicillin, and 100mg/ml streptomycin. The SUM149 cell line was validated by STR DNA fingerprinting using the AmpF_STR identifier kit following the manufacturer's protocol (Applied Biosystems cat 4322288). The STR profiles were compared to ATCC fingerprints (ATCC.org) and the Cell Line Integrated Molecular Authentication (CLIMA) database version 0.1.200808 (<http://bioinformatics.istge.it/clima/>) (38). The PARP inhibitor-resistant triple-negative breast cancer cell lines, B3 and C12, were obtained from MK Chen and cultured as per SUM149.

2.2 Immunoblotting

Whole cell lysates were prepared in radioimmunoprecipitation (RIPA) buffer (20 mM Tris-HCl, pH 7.5, 150 mM NaCl, 1mM Na₂EDTA, 1mM EGTA, 1% NP-40, 1% sodium deoxycholate, 2.5 mM sodium pyrophosphate, 1 mM β -glycerophosphate, 1mM Na₃VO₄, 1 μ g/ml leupetin) with protease inhibitors (bimake.com) and phosphatase inhibitors (biotool.com). The concentration of protein in whole cell lysates was determined using the Pierce BCA protein assay kit (Fisher PI-23227) according to the manufacturer's protocol. 10-40 μ g of protein from each sample was separated in an 8% Bis-Tris SDS PAGE gel and transferred to a polyvinylidene difluoride (PVDF) membrane (Life Technologies). After blocking with 5% bovine serum albumin (BSA), primary antibodies were incubated with the PVDF membranes overnight at 4°C. Membranes were washed in TBST (50 mM Tris-Cl, pH

7.5, 150 mM NaCl, 0.05% Tween-20) and hybridized with appropriate secondary antibodies for 45 minutes at room temperature and imaged using ECL reagents (Bio-Rad Laboratories).

2.3 Immunoprecipitation

Whole cell lysates were prepared in immunoprecipitation buffer (25 mM Tris, pH 7.4; 150 mM NaCl, 0.1% NP-40, 1 mM EDTA, 10% glycerol) and incubated with 1 µg of primary antibody or IgG control antibody overnight at 4°C. Protein G-agarose beads were then added and incubated at 4°C for 1 hour prior to washing and detection by immunoblotting as described in the previous section.

2.4 MTT assay

B3 cells (1250 cells/well) and C12 cells (750 cells/well) were seeded in a 96 well plate and incubated overnight. After 24 hours, cells were then treated with varying concentrations of talazoparib and/or crizotinib for 6 days. 3-(4,5-dimethylthiazol-2-yl)-2,5-diphenyltetrazolium bromide (MTT) was added into each well to achieve a final concentration of 0.5 µg/ml before formazan extraction with DMSO. The optical density at 590 nm in each well was measured and then normalized to untreated wells. The Chou-Talalay method (39) was used to calculate the combination index using the Compusyn software (<http://www.combosyn.com>).

2.5 Plasmids and transfection

For knockdown of c-MET, the PARP inhibitor-resistant triple-negative breast cancer cell lines, B3 and C12, were transfected with pLKO-shRNA vector (Sigma-Aldrich, St. Louis, MO). shRNA sequences used in generating stable knockdown clones are as follows (5' to 3'):

CCGGGTGTGTTGTATGGTCAATAACCTCGAGGTTATTGACCATACAACACACTTT
TTTG*;

CCGGCCTTCAGAAGGTTGCTGAGTACTCGAGTACTCAGCAACCTTCTGAAGGTTT
TTG

*Targeting the 3' UTR:

2.6 Chemicals and Antibodies

Olaparib and talazoparib were purchased from Selleck Chemical (Houston, TX), Crizotinib was purchased from LC laboratories. Antibodies against MET (#8198), phospho-MET (#3077), EGFR (#4267) and IgG (#2729) were purchased from Cell Signaling Technology (Danvers, MA). Antibodies for EphA2 (sc-398832) and Lamin B (sc-365962) were purchased from Santa Cruz Biotechnology (Santa Cruz, CA). The antibody for phospho-EGFR (Ab5650) was purchased from Abcam (Cambridge, UK). The antibody against ErbB2 (#OP15) and ALK (#ABN263) were purchased from Millipore Sigma (Burlington, MA). The antibody against PARP1 pY907 was obtained from China Medical University (Taichung, Taiwan) (35).

2.7 BRCA1/2 mutated breast cancer tissue samples

Tissue samples from 19 patients with stage I-III breast cancer and a germline *BRCA1/2* mutation were obtained at baseline and at the time of surgery following treatment with talazoparib in the neoadjuvant setting. Reverse phase protein arrays (40) and whole exome sequencing were performed by the proteomics and sequencing core facility at The University of Texas MD Anderson Cancer Center, respectively.

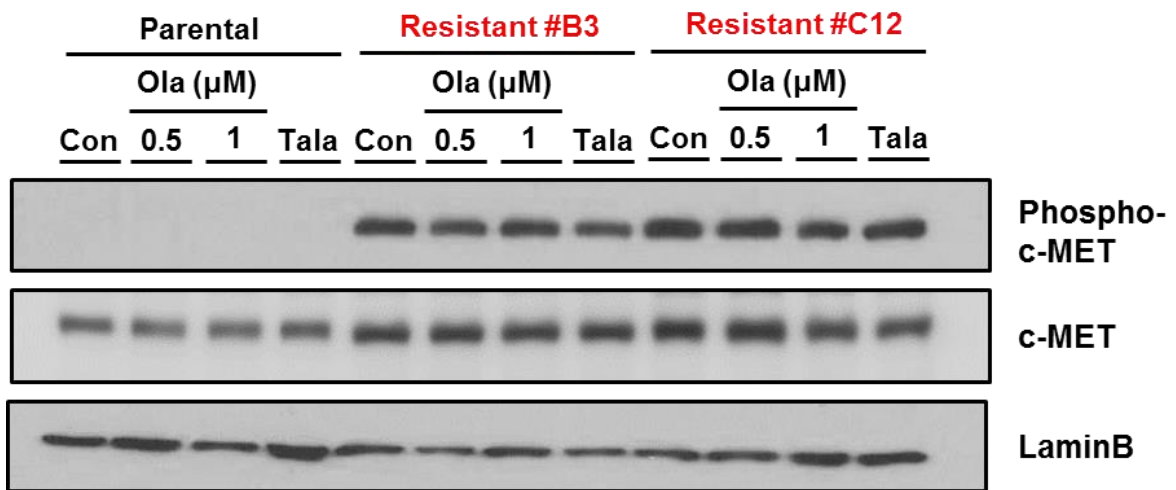
CHAPTER 3. RESULTS

3.1 Phospho-c-MET expression is higher in PARP inhibitor-resistant triple-negative breast cancer cells compared to PARP inhibitor-sensitive triple-negative breast cancer cells.

PARP inhibitor-resistant triple-negative breast cancer cell lines were created by treating a PARP inhibitor-sensitive triple-negative breast cancer cell line (SUM149) with increasing doses of the PARP inhibitor, talazoparib. 31 single clones demonstrating increased resistance to PARP inhibitors (elevated IC₅₀) were selected. Among these 31 clones, we identified two PARP inhibitor-resistant triple-negative breast cancer cell lines (B3 and C12) which had significantly higher levels of phospho-c-MET expression relative to the parental PARP inhibitor-sensitive triple-negative breast cancer cell line (SUM149) under basal conditions as well as following 24 hours of exposure to either olaparib or talazoparib (Figure 1). Total c-MET expression was also higher in the two PARP inhibitor-resistant triple-negative breast cancer cell lines (B3 and C12) compared to the parental PARP inhibitor-sensitive triple-negative breast cancer cell line (SUM149), albeit to a lesser extent (Figure 1). Therefore, the extent of c-MET phosphorylation in the PARP inhibitor-resistant triple-negative breast cancer cell lines B3 and C12 is significantly greater compared to that of the parental PARP inhibitor sensitive triple-negative breast cancer cell line (SUM149), suggesting that c-MET may play a role in mediating acquired resistance to PARP inhibitors.

FIGURE 1. The PARP inhibitor-resistant triple-negative breast cancer cell lines B3 and C12 have higher levels of phospho-c-MET expression relative to the PARP inhibitor-sensitive parental triple-negative breast cancer cell line, SUM149 (parental). Cells were treated with vehicle control (con), olaparib (ola) at a concentration of 0.5 μ M or 1.0 μ M, or talazoparib (Tala) at a concentration of 25 nM for 24 hours prior to preparation of whole cell lysates. Immunoblotting was used to determine relative levels of phospho-c-MET, total c-MET and lamin B expression.

FIGURE 1.



3.2 Combining crizotinib with talazoparib results in synergistic inhibition of cellular proliferation in PARP inhibitor-resistant triple-negative breast cancer cell lines.

The PARP inhibitor-resistant triple-negative breast cancer cell lines B3 and C12 were treated with varying concentrations of crizotinib, a multi-kinase inhibitor that inhibits c-MET, and talazoparib, a PARP inhibitor (Table 1). Using the combination index theorem of Chou-Talalay (39), the combination index for crizotinib and talazoparib was calculated. In both PARP inhibitor-resistant triple-negative breast cancer cell lines B3 and C12, the combination index for crizotinib and talazoparib was <1 at a wide range of concentrations, suggesting synergistic inhibition of cellular proliferation (Figure 2).

3.3 Depleting c-MET in PARP inhibitor-resistant triple-negative breast cancer cells has limited impact on restoring sensitivity to talazoparib.

To specifically assess the role of c-MET in acquired resistance to PARP inhibitors in triple-negative breast cancer, we depleted c-MET in two PARP inhibitor-resistant triple-negative breast cancer cell lines (B3 and C12) with significantly higher levels of phospho-c-MET expression relative to parental PARP inhibitor-sensitive triple-negative breast cancer cells using two independent short hairpin RNAs (shRNAs) which we delivered via a lentiviral system. (Figure 3). Knockdown efficiency of $>50\%$ was achieved in all cases (Figure 4). We then treated the c-MET depleted PARP inhibitor-resistant triple-negative breast cancer cell lines and c-MET expressing (vector control) PARP inhibitor-resistant triple-negative breast cancer cell lines with varying concentrations of talazoparib. Depleting c-MET in the PARP inhibitor-resistant triple-negative breast cancer cell line, C12, modestly increased sensitivity to talazoparib (Figure 5) whereas depleting c-MET in the PARP inhibitor-resistant triple-

negative breast cancer cell line, B3, did not consistently increase sensitivity to talazoparib (Figure 6).

TABLE 1. A table showing the concentrations (in nM) of crizotinib and talazoparib used in the determination of the combination index for the PARP inhibitor-resistant triple-negative breast cancer cell lines, B3 and C12.

TABLE 1.

| nM | Crizotinib | 250 | 500 | 1000 | 2000 | 4000 |
|-------------|------------|------|------|------|------|------|
| Talazoparib | 0 | 0 | 0 | 0 | 0 | 0 |
| 62.5 | 62.5 | 62.5 | 62.5 | 62.5 | 62.5 | 62.5 |
| 125 | 125 | 125 | 125 | 125 | 125 | 125 |
| 250 | 250 | 250 | 250 | 250 | 250 | 250 |
| 500 | 500 | 500 | 500 | 500 | 500 | 500 |
| 1000 | 1000 | 1000 | 1000 | 1000 | 1000 | 1000 |

FIGURE 2. The combination of crizotinib and talazoparib results in synergistic inhibition of cellular proliferation in PARP inhibitor-resistant triple-negative breast cancer cell lines, B3 and C12. The PARP inhibitor-resistant triple-negative breast cancer cell lines, B3 and C12, were treated with varying concentrations of crizotinib and talazoparib for 6 days. Following 6 days of treatment, the 3-(4,5-dimethylthiazol-2-yl)-2,5-diphenyltetrazolium bromide (MTT) assay was performed. The combination index (CI) was calculated and synergistic inhibition of cellular proliferation was defined as a CI <1.

FIGURE 2.

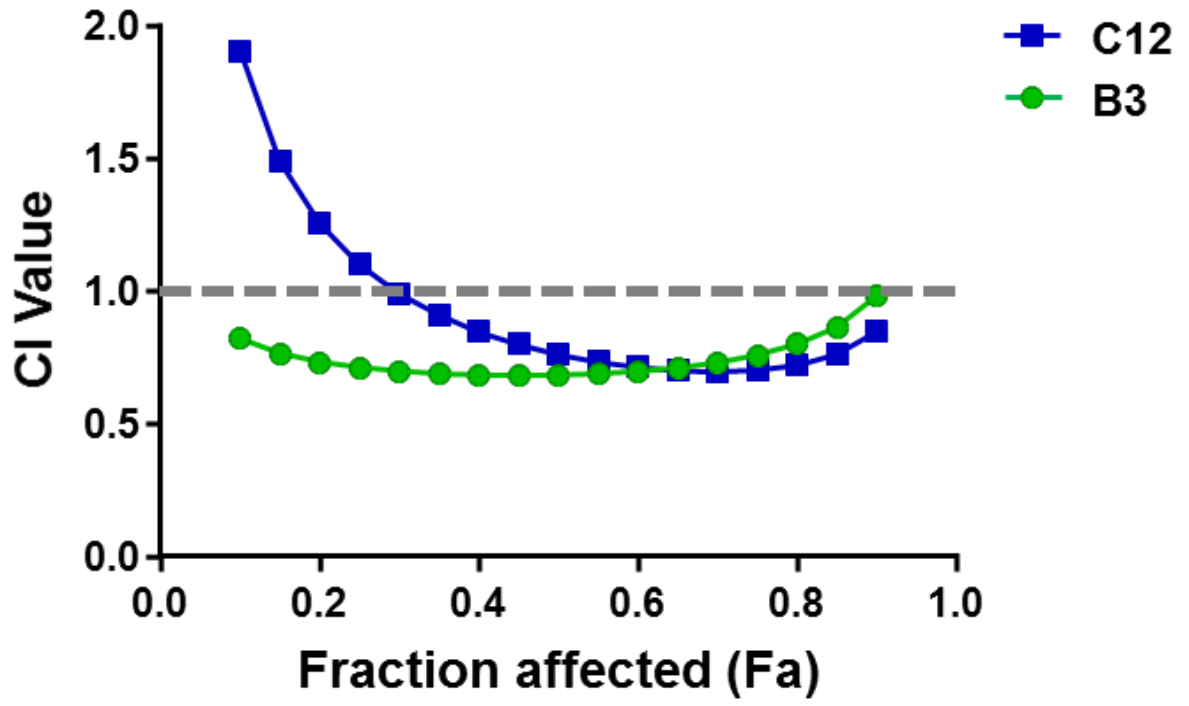


FIGURE 3. PARP inhibitor-resistant triple-negative breast cancer cell lines were infected with lentiviral particles carrying non-specific or c-MET-targeting short harpin RNA (shRNAs) sequences.

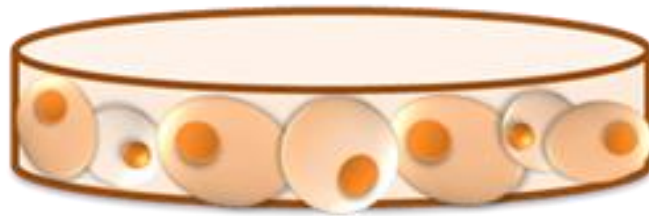
FIGURE 3.



shRNA knock-down



Virus infection



Puromycin selection

FIGURE 4. Following lentiviral delivery of two independent short harpin RNAs targeting c-MET to PARP inhibitor-resistant triple-negative breast cancer cell lines, B3 and C12, expression levels of c-MET was reduced by at least 50% relative to cells receiving non-specific short hairpin RNA (shRNA) sequences. The PARP inhibitor-resistant triple-negative breast cancer cell lines, B3 and C12, were infected with control shRNA (control), an shRNA targeting the 3' UTR of c-MET (sh-c-MET-1), or an shRNA targeting the coding region of c-MET (sh-c-MET-2). Relative expression levels of total c-MET in stable clones were determined by immunoblotting.

FIGURE 4.

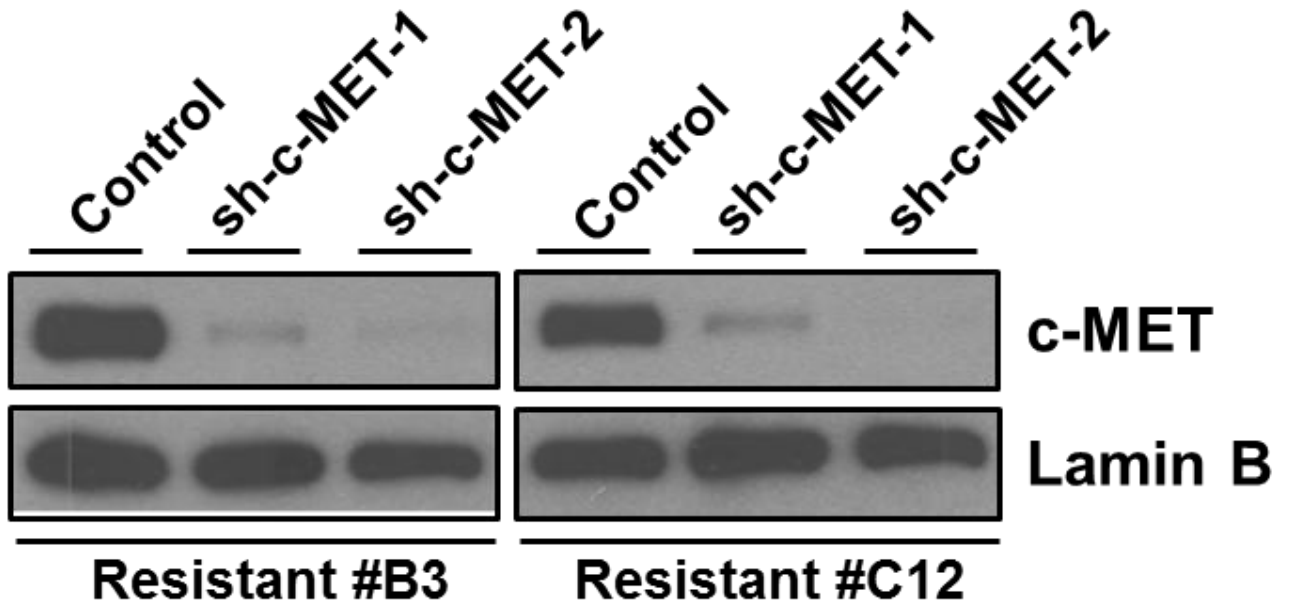


FIGURE 5. Depleting c-MET results in a modest increase in sensitivity to talazoparib in the PARP inhibitor-resistant triple-negative breast cancer cell line C12. 750 cells were seeded in each well of a 96-well plate on Day 0. On Day 1, talazoparib was added at varying concentrations to each well (12.5-200 nM). Following 6 days of treatment, the 3-(4,5-dimethylthiazol-2-yl)-2,5-diphenyltetrazolium bromide (MTT) assay was performed and the percentage of surviving cells in each well was calculated. Depicted values represent the mean of biological and technical triplicates.

FIGURE 5.

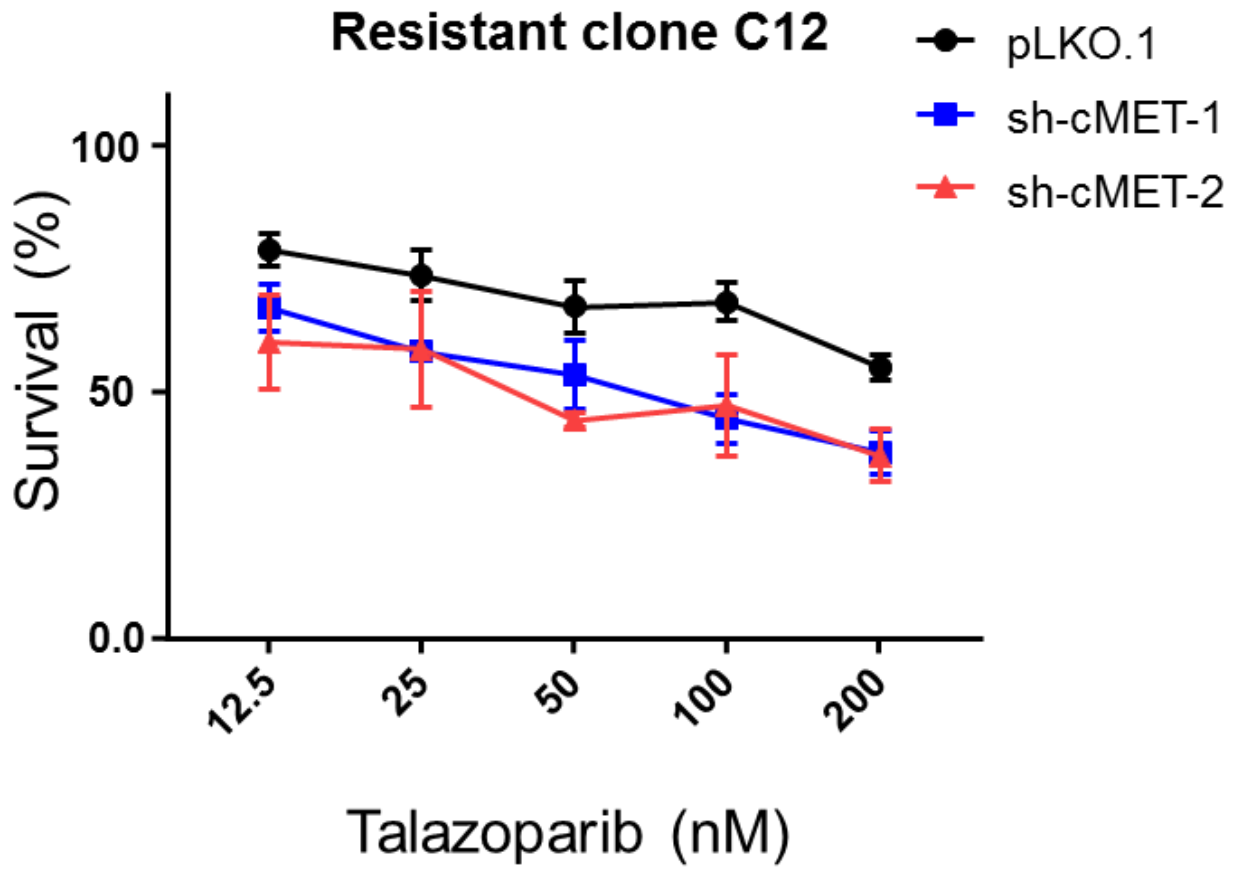
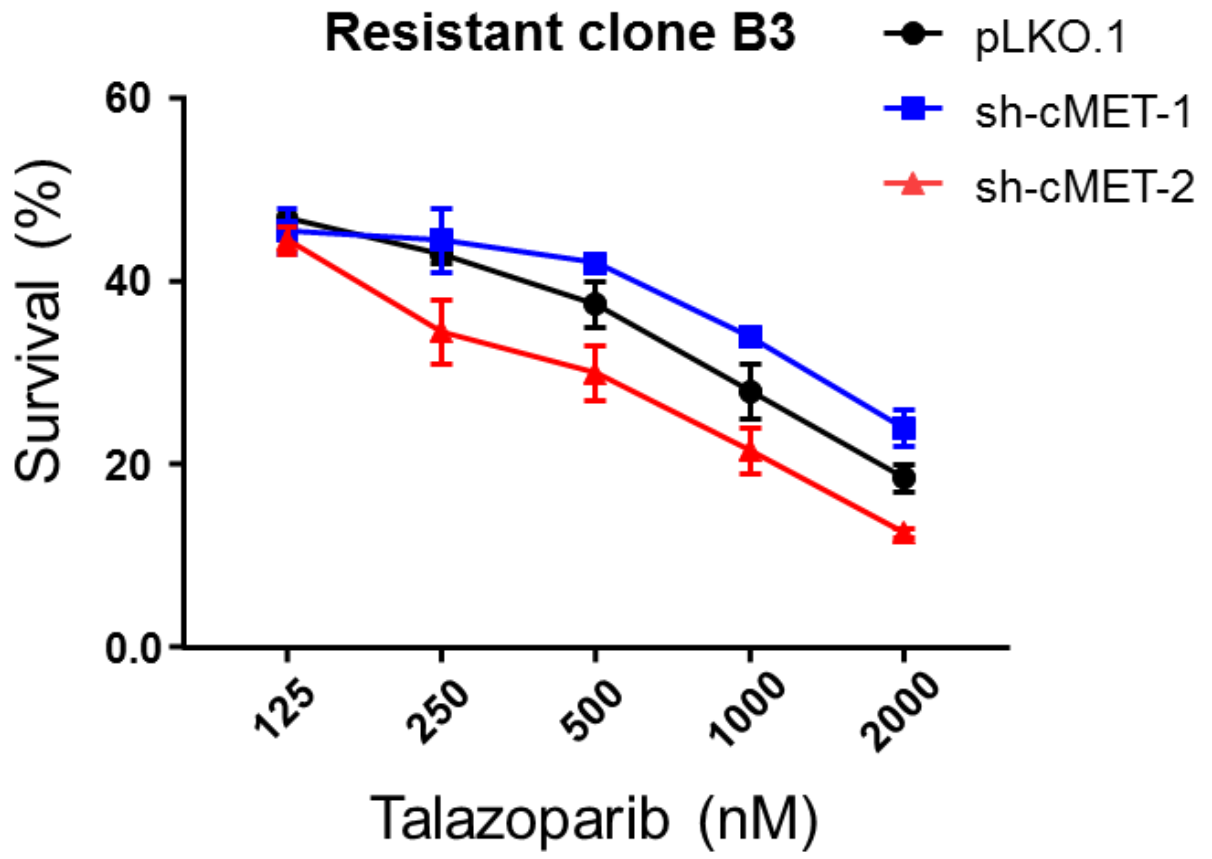


FIGURE 6. Depleting c-MET in the PARP inhibitor resistant triple-negative breast cancer cell line B3 does not consistently increase sensitivity to talazoparib. 1500 cells were seeded in each well of a 96-well plate on Day 0. On Day 1, talazoparib was added at varying concentrations to each well (125-2000 nM). Following 6 days of treatment, the 3-(4,5-dimethylthiazol-2-yl)-2,5-diphenyltetrazolium bromide (MTT) assay was performed and the percentage of surviving cells in each well was calculated. Depicted values represent the mean of biological and technical triplicates.

FIGURE 6.



3.4 c-MET interacts with EGFR in PARP inhibitor-resistant triple-negative breast cancer cell lines.

Since c-MET is known to interact with multiple cell surface molecules (41), including receptor tyrosine kinases like EGFR (41), we evaluated expression data derived from a phospho-receptor tyrosine kinase array comparing expression levels of a series of phospho-receptor tyrosine kinases in the PARP inhibitor-resistant triple-negative breast cancer cell line, C12, to that in the PARP inhibitor-sensitive parental triple-negative breast cancer cell line, SUM149 (data not shown). Following exposure to talazoparib, the phospho-c-MET overexpressing PARP inhibitor-resistant triple-negative breast cancer cell line, C12, was found to have higher expression levels of phospho-EGFR, phospho-ErbB2, phospho-ALK, and phospho-EPHA2 relative to the PARP inhibitor-sensitive parental triple-negative breast cancer cell line, SUM149 (data not shown). We therefore hypothesized that the modest effect of c-MET depletion on talazoparib sensitivity in PARP inhibitor-resistant triple-negative breast cancer cell lines could be the result of protein-protein interactions involving c-MET and other receptor tyrosine kinases. To identify potential c-MET interacting receptor tyrosine kinases, we immunoprecipitated c-MET, and found enhanced interaction between c-MET and EGFR in the PARP inhibitor-resistant triple-negative breast cancer cell line, C12, relative to the PARP inhibitor-sensitive parental triple-negative breast cancer cell line, SUM149 (Figure 7). In contrast, ErbB2 (Figure 7), ALK (Figure 8) and EphA2 (Figure 8) were not identified as interacting proteins of c-MET. We then immunoprecipitated c-MET in whole cell lysates obtained from the PARP inhibitor-resistant triple-negative breast cancer cell lines, B3 and C12, as well as PARP inhibitor-sensitive triple-negative breast cancer cell line (SUM149) under basal conditions and following treatment with talazoparib. The results showed that the

interaction between c-MET and EGFR was enhanced in the PARP inhibitor-resistant cells relative to the PARP inhibitor-sensitive parental cells under basal conditions as well as following treatment with talazoparib (Figure 9). In addition, expression of phospho- and total-EGFR was significantly higher in PARP inhibitor-resistant triple-negative breast cancer cell lines, B3 and C12, compared to the PARP inhibitor-sensitive parental triple-negative breast cancer cell line, SUM149, under basal conditions as well as following 24 hours of treatment with olaparib or talazoparib (Figure 10). Collectively, these data suggest that EGFR may cooperate with c-MET in mediating resistance to PARP inhibitors through direct interaction.

FIGURE 7. Enhanced interaction between c-MET and EGFR but not ErbB2 is detected in the PARP inhibitor-resistant triple-negative breast cancer cell line, C12, relative to PARP inhibitor-sensitive parental (PT) triple-negative breast cancer cell line (SUM149), following treatment with talazoparib. Parental (PT) cells and resistant cell (C12) were treated with talazoparib (Tala) at a concentration of 25 nM for 24 hours prior to preparation of whole cell lysates. Anti-cMET or IgG control antibodies were used to immunoprecipitate the cell lysate. EGFR and ErbB2 expression was then analyzed by immunoblotting.

FIGURE 7.

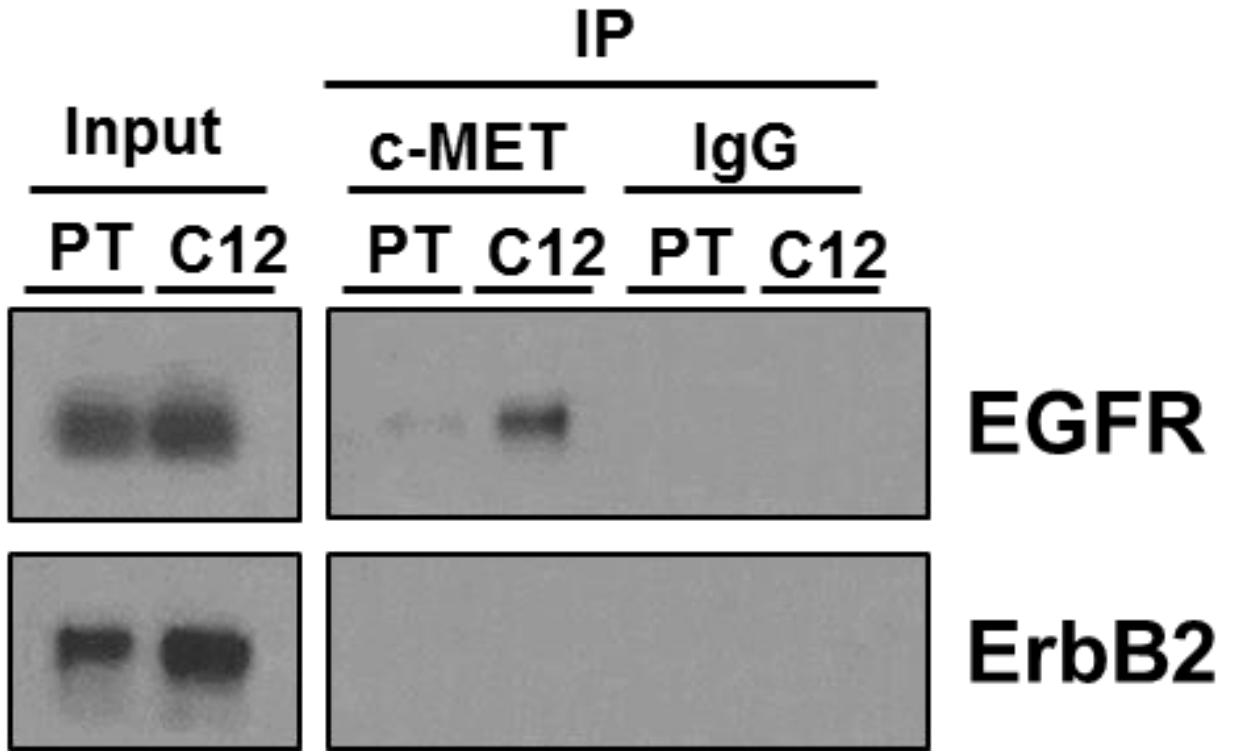


FIGURE 8. Interaction between c-MET and ALK or EphA2 was not enhanced in the PARP inhibitor-resistant triple-negative breast cancer cell, C12, relative to PARP inhibitor-sensitive parental (PT) triple-negative breast cancer cells (SUM149), following treatment with talazoparib. Parental (PT) cells and resistant cell (C12) were treated with talazoparib (Tala) at a concentration of 25 nM for 24 hours prior to preparation of whole cell lysates. Anti-cMET or IgG control antibodies were used to immunoprecipitate the cell lysate. ALK and EphA2 expression was then analyzed by immunoblotting.

FIGURE 8

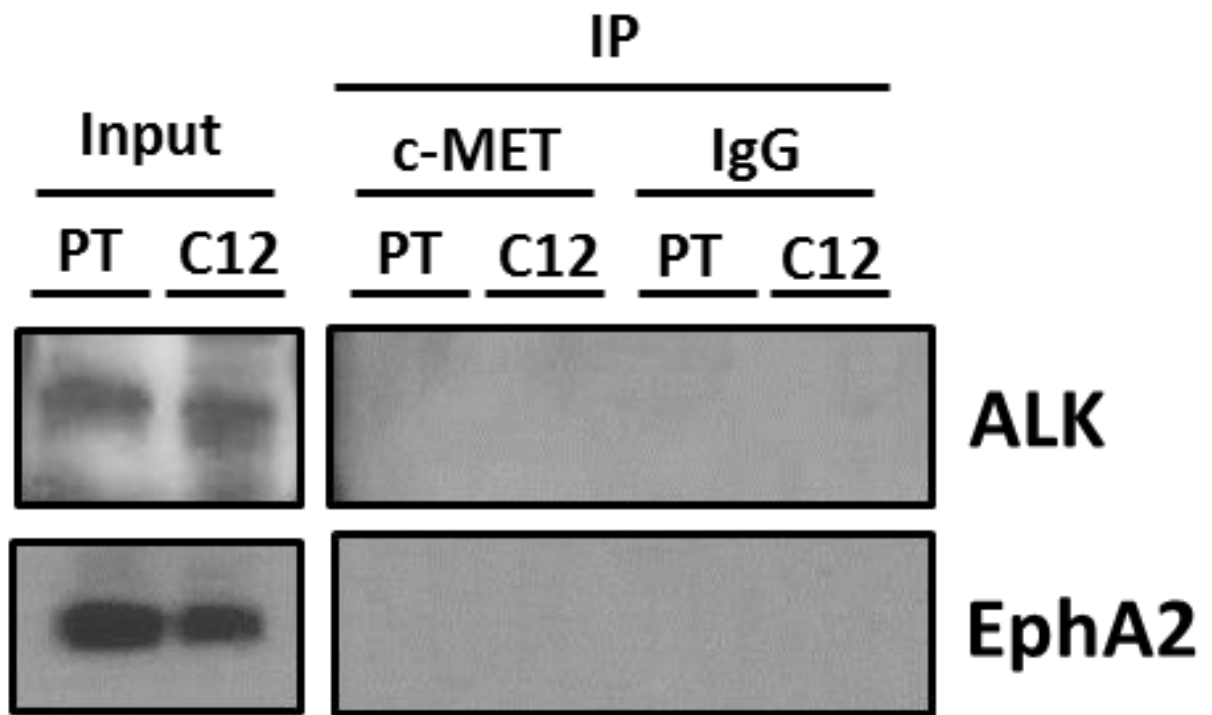


FIGURE 9. The interaction between c-MET and EGFR is enhanced in PARP inhibitor-resistant triple-negative breast cancer cells (B3 and C12) relative to PARP inhibitor-sensitive parental (PT) triple-negative breast cancer cells (SUM149), under basal conditions as well as following treatment with talazoparib. Parental (PT) cells and resistant cells (B3 and C12) were treated with vehicle control (Con) or talazoparib (Tala) at a concentration of 25 nM for 24 hours prior to preparation of whole cell lysates. Anti-cMET or IgG control antibodies were used to immunoprecipitate the cell lysate. EGFR expression was then analyzed by immunoblotting.

FIGURE 9

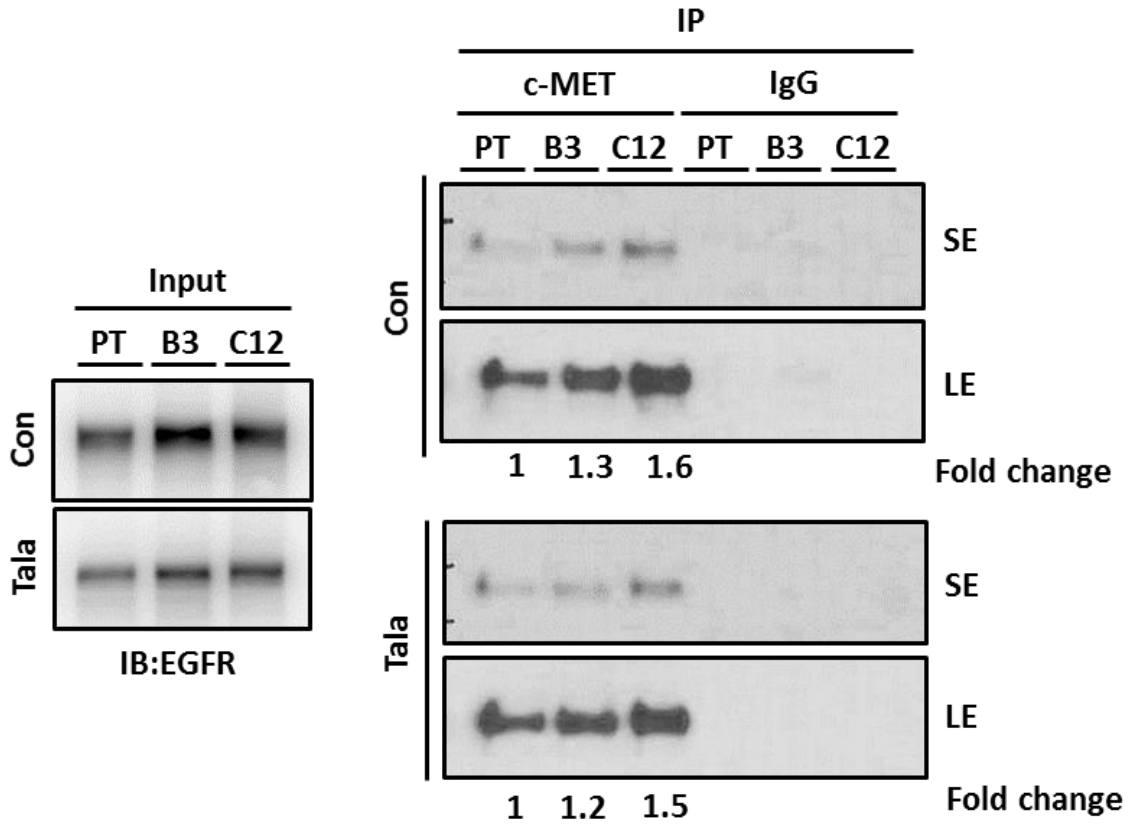
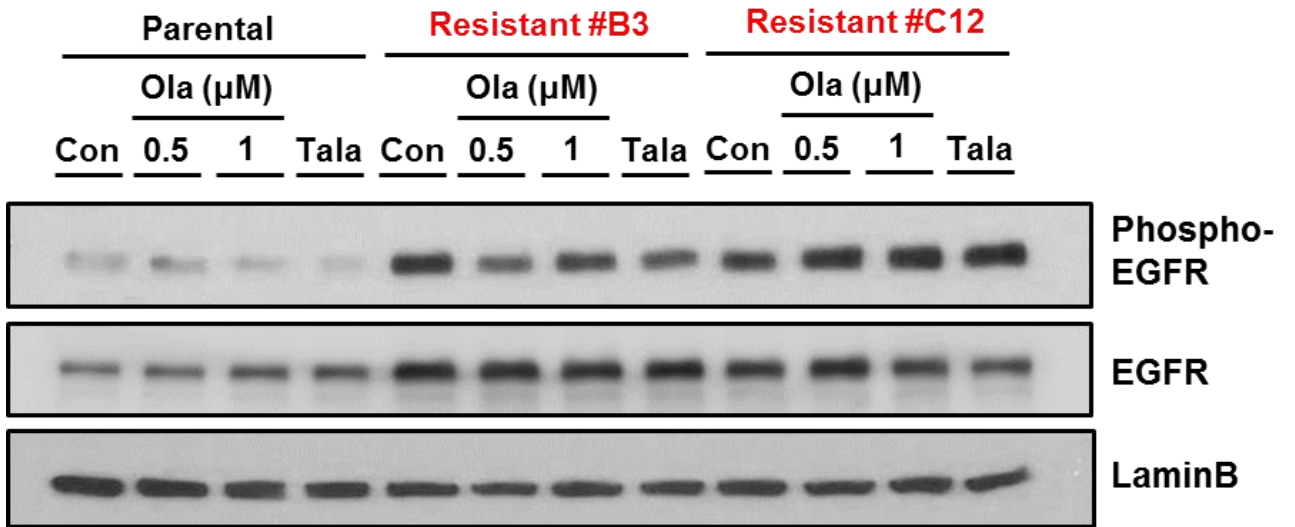


FIGURE 10. The PARP inhibitor-resistant triple-negative breast cancer cell lines B3 and C12 have higher levels of phospho- and total-EGFR expression relative to the PARP inhibitor-sensitive parental triple-negative breast cancer cell line, SUM149. Cells were treated with vehicle control, olaparib at a concentration of 0.5 μ M or 1.0 μ M, or talazoparib at a concentration of 25 nM for 24 hours prior to preparation of whole cell lysates. Relative expression levels of phospho- and total-EGFR were determined by immunoblotting.

FIGURE 10.



3.5 c-MET and EGFR/phospho-EGFR protein expression levels increase in patients with talazoparib-resistant breast cancer.

We identified 19 patients with previously untreated stage I-III breast cancer who received talazoparib in the neoadjuvant setting as part of a clinical trial conducted at The University of Texas MD Anderson Cancer Center (NCT02282345). Patients enrolled on this study underwent a pretreatment core needle biopsy at baseline and received up to 6 months of treatment with talazoparib before undergoing surgery to remove any residual cancer (Figure 11). The amount of residual cancer was quantified using the residual cancer burden (RCB) index (42). Patients were classified as having talazoparib-sensitive disease if they had a pathologic complete response or minimal residual disease (pCR/RCB-I) and classified as having talazoparib-resistant disease if they had significant residual disease (RCB-II/RCB-III). Of the 19 patients, 4 patients had sufficient tissue for paired analysis. Among the 4 patients with paired tissue samples, 2 had talazoparib-sensitive disease and the remaining 2 had talazoparib-resistant disease. Following treatment with talazoparib, patients with talazoparib-sensitive disease had a decrease in c-MET, EGFR and phospho-EGFR protein expression, whereas patients with talazoparib-resistant disease had an increase in c-MET, EGFR and phospho-EGFR protein expression (Figures 12-14), suggesting potential compensatory upregulation of these pathways in talazoparib-resistant breast cancer.

3.6 Genomic alterations in c-MET and EGFR in patients treated with talazoparib

Whole exome sequencing was performed on baseline and surgical specimens obtained from the 19 patients with stage I-III breast cancer treated with talazoparib in the neoadjuvant setting. We did not identify any single nucleotide variants or indels in MET or EGFR in tumors

from this cohort of patients. Baseline MET copy number was similar in tumors from patients with talazoparib-sensitive and talazoparib-resistant disease (Figure 15). Among the 4 patients with paired samples, treatment with talazoparib increased MET copy number (Figure 15 but the greatest difference was observed in patients with talazoparib-resistant disease. Interestingly, patients who had talazoparib-sensitive disease appeared to have higher EGFR copy number compared to patients who had talazoparib-resistance disease at baseline (Figure 16). Among the 4 patients with paired samples, treatment with talazoparib treatment with talazoparib increased EGFR copy number (Figure 16) but the greatest difference was observed in patients with talazoparib-resistant disease.

FIGURE 11. Study schema for NCT02282345. Patients with stage I-III breast cancer with a germline *BRCA1* or *BRCA2* mutation underwent a pretreatment core needle biopsy at baseline. Patients were then treated with up to 6 months of talazoparib prior to definitive surgery to remove any residual cancer.

FIGURE 11.

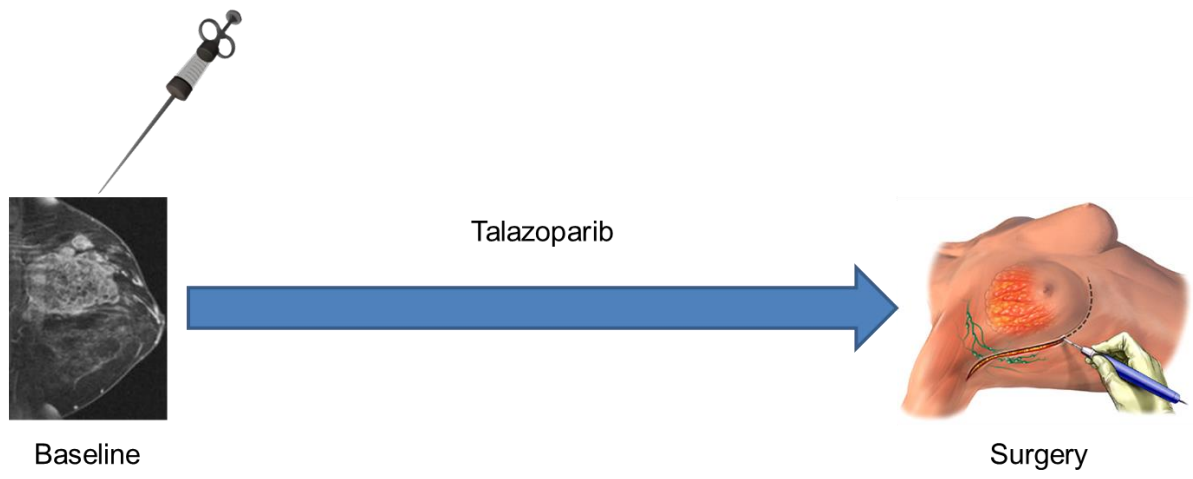


FIGURE 12. MET protein expression increased in patients with talazoparib-resistant breast cancer following treatment with single-agent talazoparib in the neoadjuvant setting. Patients with stage I-III breast cancer with a germline *BRCA1/2* mutation were treated with talazoparib in the neoadjuvant setting prior to undergoing definitive surgery. Patients underwent a baseline core needle biopsy prior to initiating therapy. Reverse phase protein arrays were used to measure levels of MET expression in pre-treatment biopsy specimens and surgical specimens obtained at the end of treatment.

FIGURE 12.

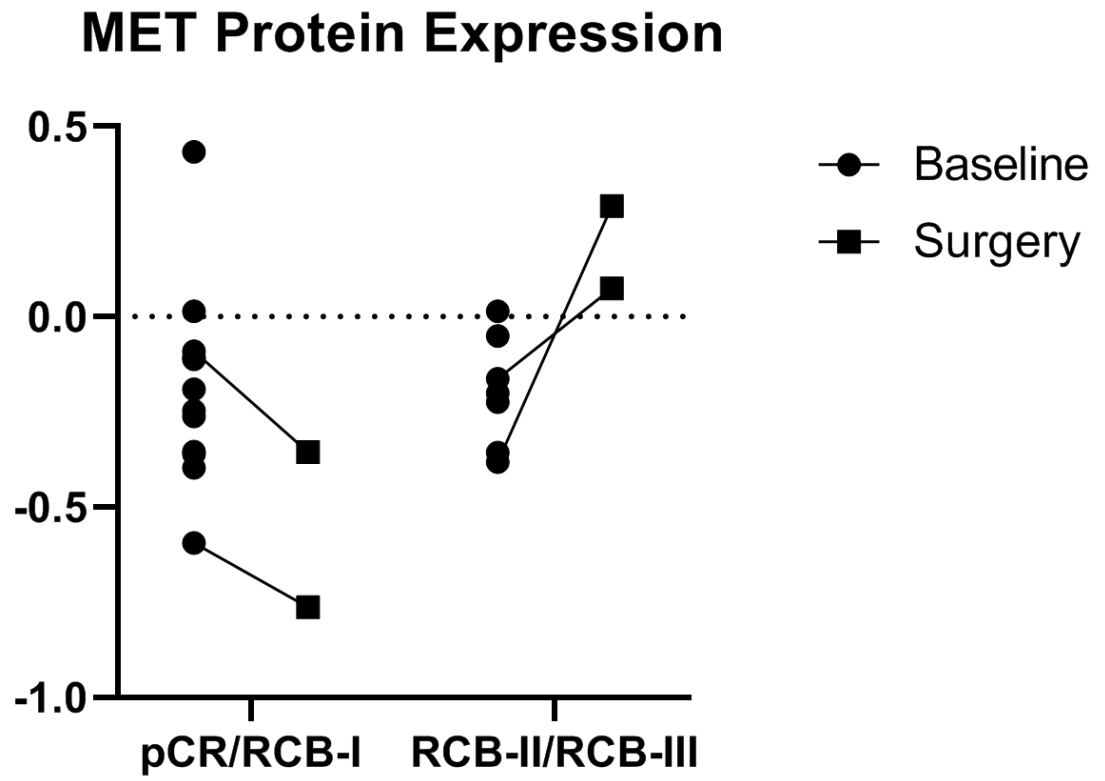


FIGURE 13. Patients with talazoparib-resistant breast cancer had an increase in EGFR expression following treatment with single-agent talazoparib in the neoadjuvant setting.

Patients with stage I-III breast cancer with a germline *BRCA1/2* mutation were treated with talazoparib in the neoadjuvant setting prior to undergoing definitive surgery. Patients underwent a baseline core needle biopsy prior to initiating therapy. Reverse phase protein arrays were used to measure levels of EGFR expression in pre-treatment biopsy specimens and surgical specimens obtained at the end of treatment.

FIGURE 13.

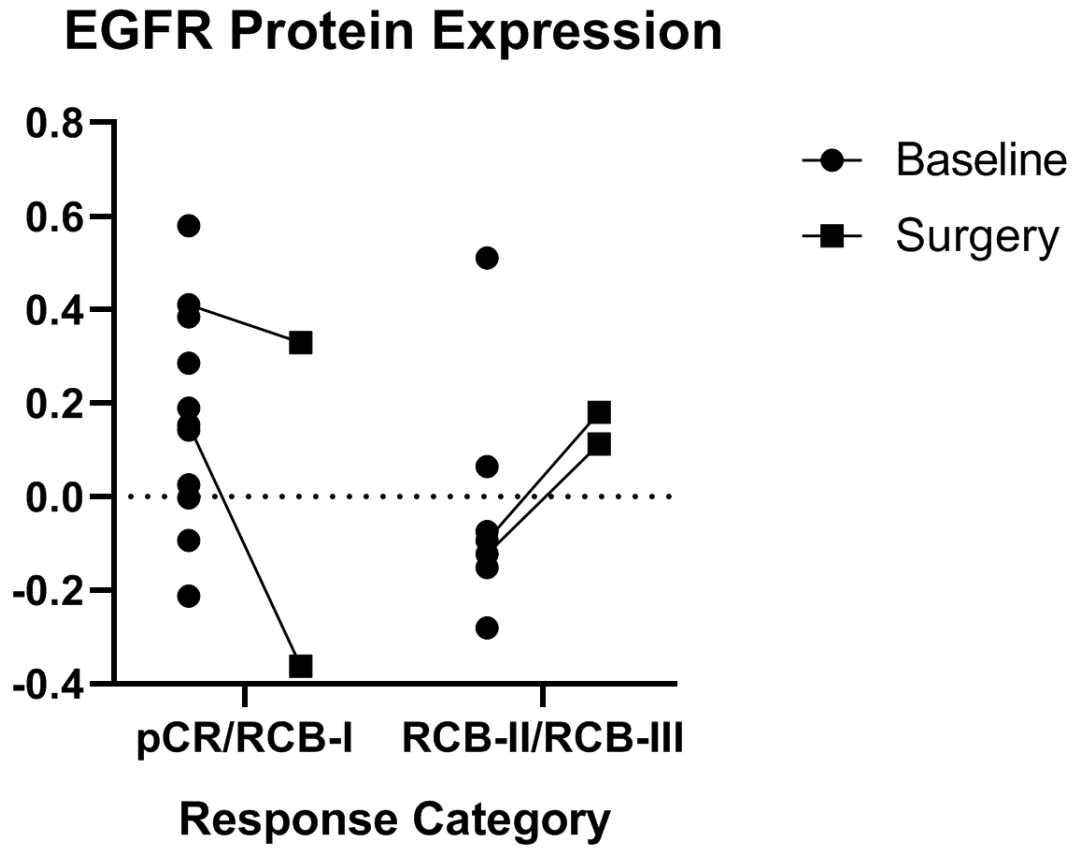


FIGURE 14. Phospho-EGFR expression levels increased in patients with talazoparib-resistant breast cancer following treatment with single-agent talazoparib in the neoadjuvant setting. Patients with stage I-III breast cancer with a germline *BRCA1/2* mutation were treated with talazoparib in the neoadjuvant setting prior to undergoing definitive surgery. Patients underwent a baseline core needle biopsy prior to initiating therapy. Reverse phase protein arrays were used to measure levels of phospho-EGFR expression in pre-treatment biopsy specimens and surgical specimens obtained at the end of treatment.

FIGURE 14.

Phospho-EGFR Protein Expression

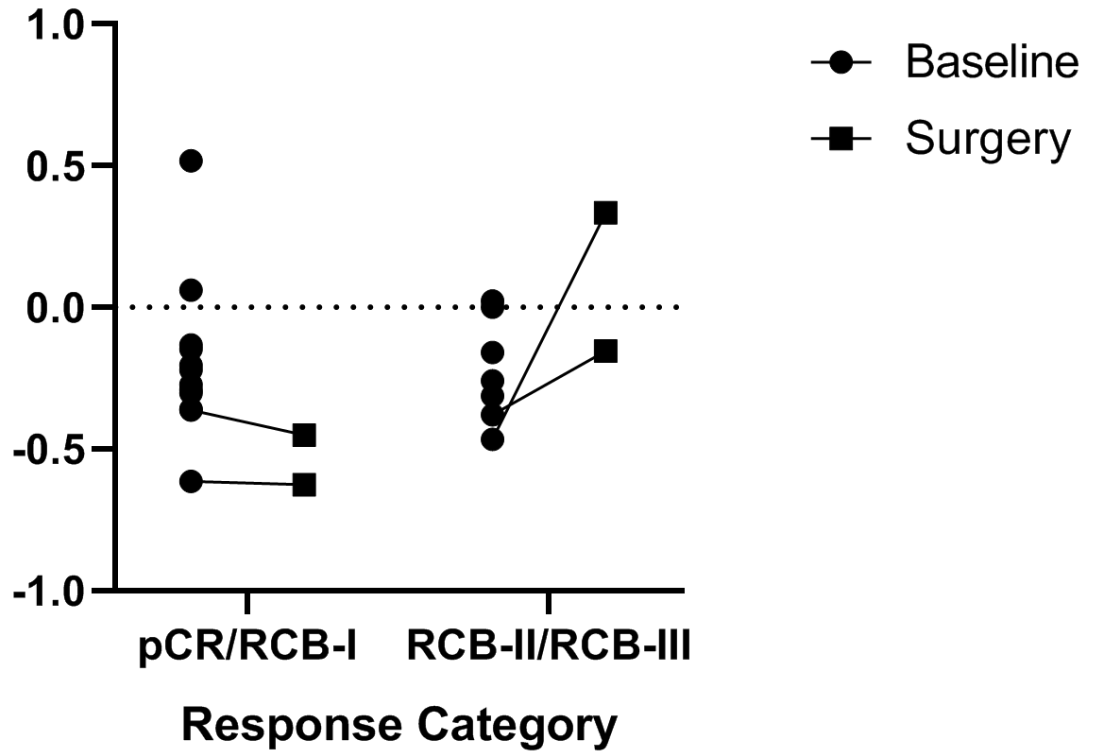


FIGURE 15. Patients with talazoparib-sensitive and talazoparib-resistant disease appeared to have similar MET copy number at baseline. Treatment with talazoparib increased MET gene copy number, with the greatest increase observed in patients with talazoparib-resistant disease. Patients with stage I-III breast cancer with a germline *BRCA1/2* mutation were treated with talazoparib in the neoadjuvant setting prior to undergoing definitive surgery. Patients underwent a baseline core needle biopsy prior to initiating therapy. Whole exome sequencing was used to determine gene copy numbers of MET in pre-treatment biopsy specimens and surgical specimens obtained at the end of treatment.

FIGURE 15.

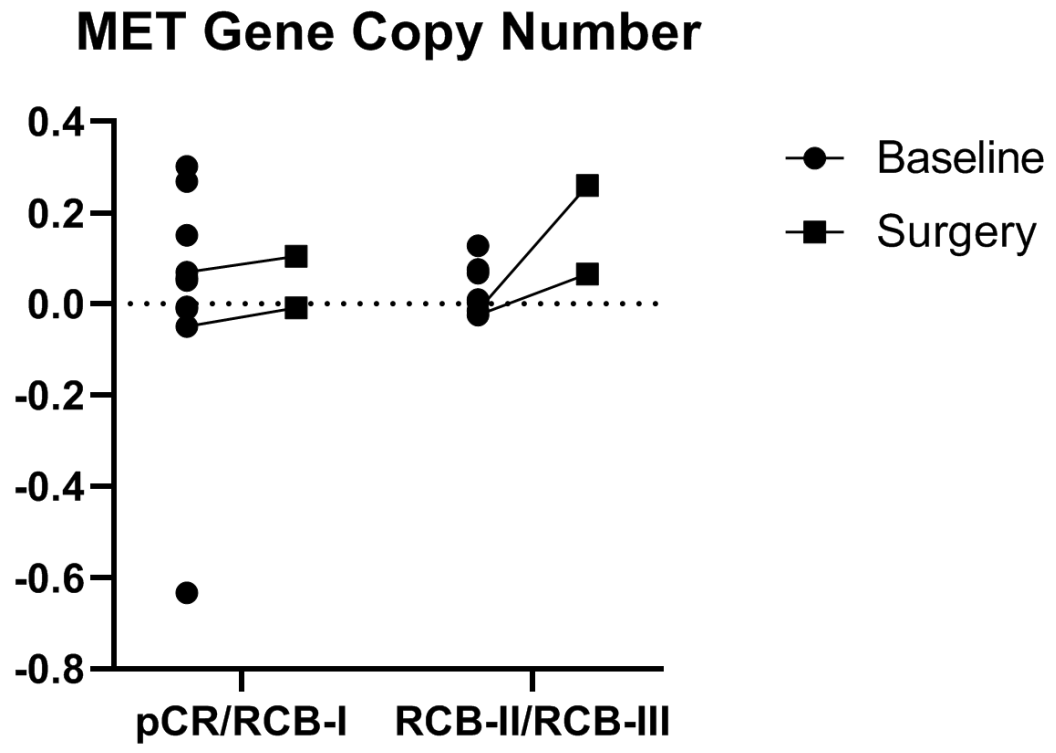
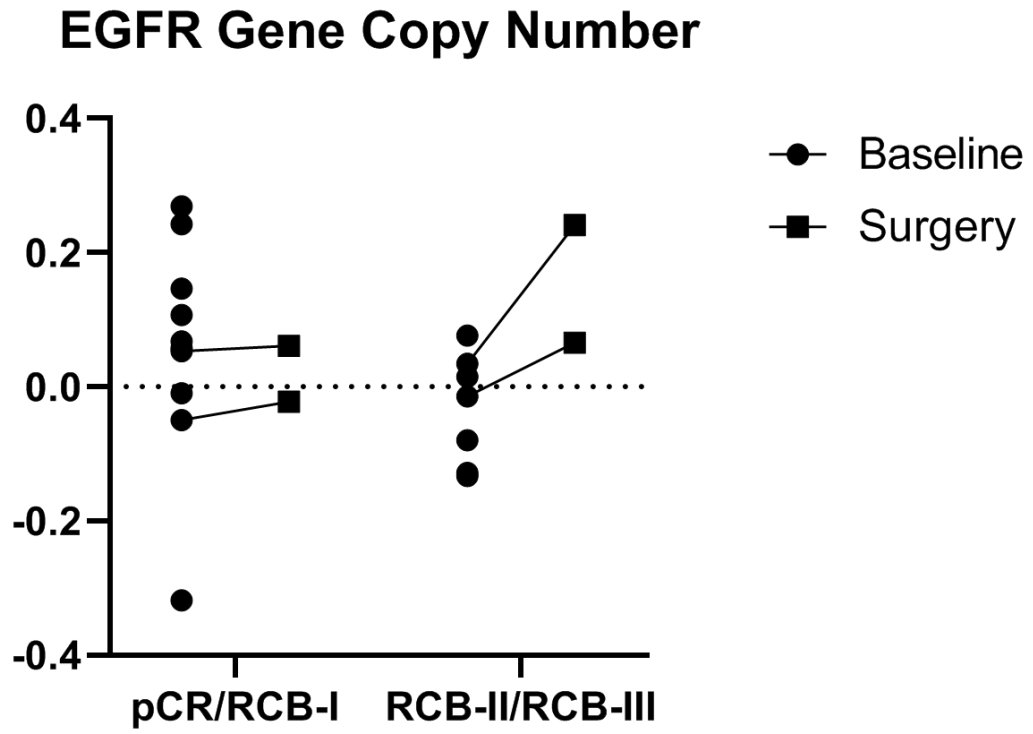


FIGURE 16. Patients with talazoparib-sensitive disease had higher EGFR copy number at baseline. Treatment with talazoparib increased EGFR gene copy number, with the greatest increase observed in patients with talazoparib-resistant disease. Patients with stage I-III breast cancer with a germline *BRCA1/2* mutation were treated with talazoparib in the neoadjuvant setting prior to undergoing definitive surgery. Patients underwent a baseline core needle biopsy prior to initiating therapy. Whole exome sequencing was used to determine gene copy numbers of EGFR in pre-treatment biopsy specimens and surgical specimens obtained at the end of treatment.

FIGURE 16.

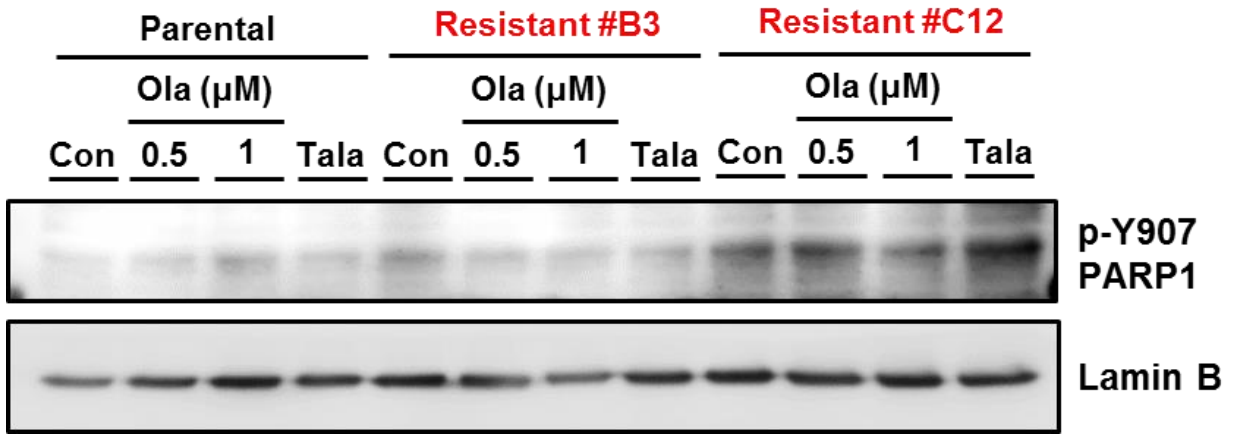


3.7 Phosphorylation of PARP1 is not observed consistently in phospho-c-MET overexpressing PARP inhibitor-resistant triple-negative breast cancer cell lines.

In a model of intrinsic resistance to PARP inhibitors in triple-negative breast cancer, it was previously demonstrated that oxidative stress increases phosphorylation of c-MET which in turn phosphorylates PARP1 at the Tyr907 residue (PARP1 pTyr907 or pY907) (35), increasing enzymatic activity of PARP1 and reducing PARP inhibitor binding (35) which leads to PARP inhibitor resistance. In addition, while preclinical studies in hepatocellular carcinoma revealed that oxidative damage led to increased PARP1 pY907 expression (36), inhibiting c-MET activity with crizotinib did not consistently reduce PARP1 pY907 expression levels in hepatocellular carcinoma cell lines due to EGFR-mediated PARP1 phosphorylation (36). Thus, since we observed evidence of increased interaction between c-MET and EGFR in the c-MET overexpressing PARP inhibitor-resistant triple-negative breast cancer cell lines, B3 and C12, relative to the PARP inhibitor-sensitive parental triple-negative breast cancer cell line, SUM149, we hypothesized that c-MET and EGFR cooperate to augment resistance to PARP inhibitors through increased phosphorylation of PARP1 at the Tyr907 residue. However, while PARP1 pY907 levels were significantly higher in the PARP inhibitor-resistant triple-negative breast cancer cell line, C12, compared to the PARP inhibitor-sensitive parental triple-negative breast cancer cell line, SUM149, PARP1 Y907 levels were not significantly higher in the second c-MET overexpressing PARP inhibitor-resistant triple-negative breast cancer cell line, B3 (Figure 17). Together, these data suggest that increased PARP1 pY907 expression is unlikely to be the dominant mechanism contributing to acquired resistance to PARP inhibitors in c-MET overexpressing triple-negative breast cancer.

FIGURE 17. p-Y907 PARP1 expression is increased in resistant cells, C12 but not B3 with PARPi treatment. PARP inhibitor-sensitive parental (PT) triple-negative breast cancer cells (SUM149) and PARP inhibitor-resistant triple-negative breast cancer cells (B3 and C12) were treated with vehicle control (Con), olaparib (Ola) at a concentration of 0.5 μ M or 1.0 μ M, or talazoparib (Tala) at a concentration of 25 nM for 24 hours prior to preparation of whole cell lysates. The cell lysates were then subjected to western blotting with the indicated antibodies.

FIGURE 17.



3.8 Interacting proteins of c-MET and EGFR are involved in DNA damage repair.

Given the observed interaction between EGFR and c-MET in c-MET overexpressing PARP inhibitor-resistant triple-negative breast cancer cell lines we sought to identify potential mechanisms of acquired resistance to PARP inhibitors in this setting, we utilized BioGRID (<https://thebiogrid.org>) and identified 91 and 1254 proteins known to interact with c-MET and EGFR, respectively. Of these, 33 were found to interact with both c-MET and EGFR (Figure 18, Table 2). Functional annotation of these 33 proteins using The Database for Annotation, Visualization and Integrated Discovery (DAVID) (<https://david.ncifcrf.gov/>) led to the identification of 6 proteins involved in DNA damage repair (Table 3).

FIGURE 18. Systematic search of a public database (BioGRID) revealed 91 c-MET interacting and 1254 EGFR-interacting proteins. Of these, 33 were identified to interact with both c-MET and EGFR.

FIGURE 18.

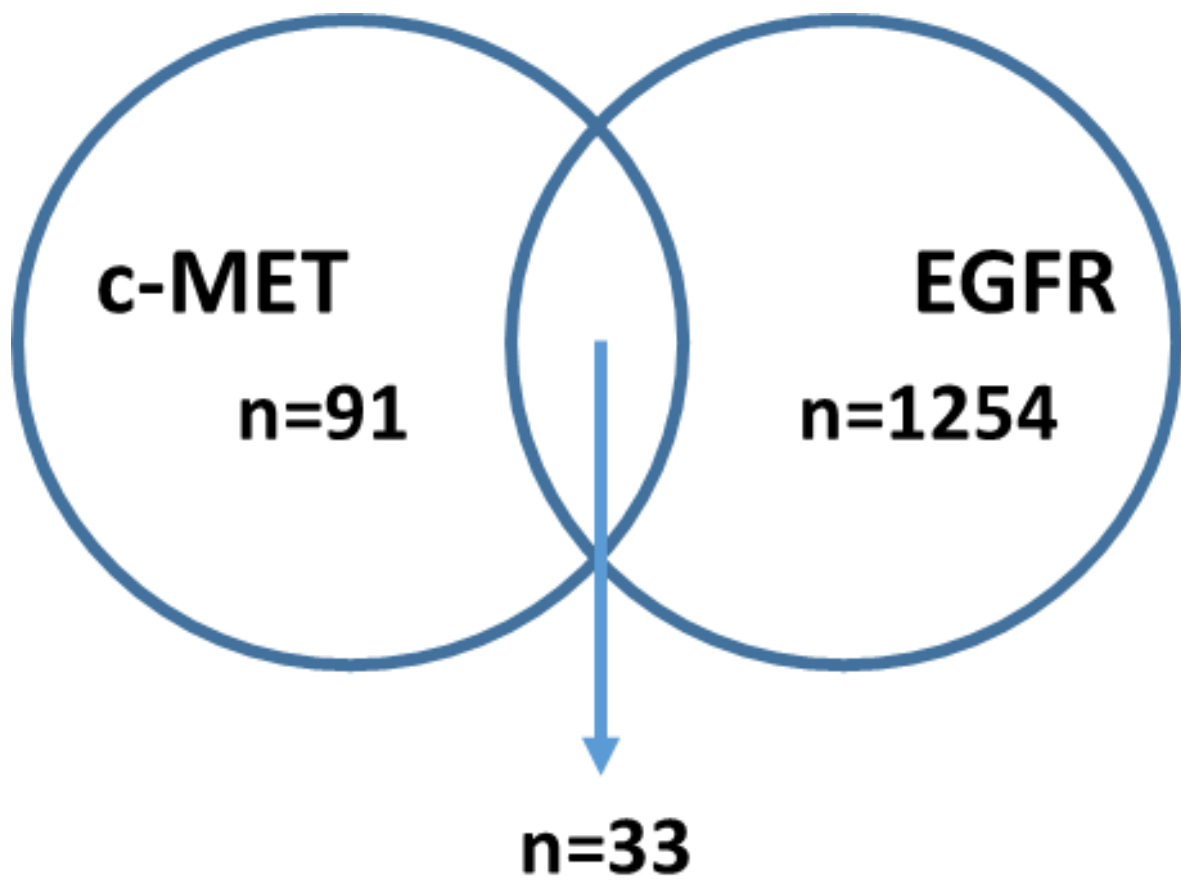


TABLE 2. List of proteins known to interact with both c-MET and EGFR.

TABLE 2.

| List of binding proteins of c-MET and EGFR | | | | | | | |
|---|--------|-------|----------|--------|--------|---------|-------|
| CBL | CRK | ERBB3 | HGS | INPPL1 | MAP2K5 | SFN | SOS1 |
| CBLC | CTNNB1 | FBXO6 | HSP90AA1 | ITGB1 | NF2 | SH3KBP1 | SRC |
| CD44 | DCN | GAB1 | HSP90AB1 | LRIG1 | PTEN | SHC1 | STAT3 |
| CDH1 | EPHA2 | GRB2 | HSPA4 | MAP2K3 | RAF1 | SOCS1 | STUB1 |
| TP53 | | | | | | | |

TABLE 3. List of proteins known to interact with both c-MET and EGFR that are involved in DNA damage repair.

TABLE 3.

| Protein/Gene | Function |
|---------------------|----------------------------------|
| FBXO6 | DNA repair |
| STUB1 | DNA repair |
| SFN | Apoptotic response to DNA damage |
| CDH1 | DNA repair |
| TP53 | DNA damage response |
| PTEN | DNA damage repair |

CHAPTER 4. DISCUSSION

4.1 Significance and Conclusions

PARP inhibitors are the first targeted agents to receive FDA approval for the treatment of triple-negative breast cancer in the setting of germline BRCA1/2 mutations. However, despite having response rates greater than double that observed with standard therapy (13, 14), the modest prolongation of median progression-free survival (13, 14) suggests the emergence of resistance shortly after an initial response. We had previously described the role of the receptor tyrosine kinase, c-MET, in a model of intrinsic resistance to PARP inhibitors using *in vitro* and *in vivo* models recapitulating BRCA1/2 wild type triple-negative breast cancers (35). However, whether c-MET plays a role in acquired resistance to PARP inhibitors in BRCA1/2-mutant triple-negative breast cancers is an unanswered question. In this study, we demonstrated that phospho-c-MET levels were higher in PARP inhibitor resistant triple-negative breast cancer cell lines compared to the PARP inhibitor-sensitive parental triple-negative breast cancer cell line. Notably, this difference in phospho-c-MET expression between PARP inhibitor-resistant triple-negative breast cancer cell lines and the PARP inhibitor-sensitive parental triple-negative breast cancer cell line was present under basal conditions as well as following treatment with olaparib or talazoparib. In contrast, oxidative stress was needed to induce phospho-c-MET expression in triple-negative breast cancer cell lines which were intrinsically resistant to PARP inhibitors (35). However, although the combination of crizotinib and talazoparib resulted in synergistic inhibition of proliferation of PARP inhibitor-resistant triple-negative breast cancer cells, depleting c-MET in these PARP inhibitor-resistant triple-negative breast cancer cells did not consistently restore sensitivity to talazoparib. Given the increased expression of additional phosphorylated receptor tyrosine

kinases in the PARP inhibitor-resistant triple-negative breast cancer cell lines and our previous work showing that EGFR interacts with c-MET to enhance resistance to PARP inhibitors in hepatocellular carcinoma (36) as well as the existence of crosstalk between c-MET and EGFR in triple-negative breast cancer (37), we systematically evaluated the existence of c-MET interacting receptor tyrosine kinases in the PARP inhibitor-resistant triple-negative breast cancer cell lines and identified EGFR as an interacting protein of c-MET in PARP inhibitor-resistant triple negative breast cancer cell lines. Notably, the observed interaction between EGFR and c-MET remained relatively consistent under both basal conditions and following treatment with talazoparib in the PARP inhibitor-resistant triple-negative breast cancer cell line, C12, but seemed to be diminished following treatment with talazoparib in the PARP-inhibitor resistant triple-negative breast cancer cell line, B3. Notably, levels of phospho-c-MET and phospho-EGFR expression in the PARP inhibitor resistant triple-negative breast cancer cell line, B3, were also diminished following treatment with talazoparib, potentially explaining the reduced interaction between c-MET and EGFR, a finding consistent with earlier data from our laboratory demonstrating that phosphorylation of c-MET and EGFR promotes their interaction (36). Of note, resistance to PARP inhibitors in hepatocellular carcinoma has been reported to be enhanced by phosphorylation of PARP1 by EGFR/MET heterodimers following oxidative DNA damage (36). In addition, inhibitors of receptor tyrosine kinases have been reported to inhibit nuclear translocation of EGFR (43) which may be necessary for EGFR/MET mediated phosphorylation of PARP1, a nuclear protein. Together, these data suggest that the interaction between EGFR and c-MET contribute to acquired resistance to PARP inhibitors in triple-negative breast cancer and combined inhibition of EGFR, c-MET

and PARP may overcome therapeutic resistance and inhibit malignant proliferation of triple-negative breast cancer.

4.2 Clinical Implications

The identification of EGFR as an interacting protein of c-MET in PARP inhibitor-resistant triple-negative breast cancer cell lines suggests that dual inhibition of c-MET and EGFR may be required to restore sensitivity to PARP inhibitors in the setting of receptor tyrosine kinase-mediated resistance. In addition, since phospho-c-MET and phospho-EGFR levels were significantly elevated in PARP inhibitor-resistant triple-negative breast cancer cell lines compared to PARP inhibitor-sensitive triple-negative breast cancer cell lines, phospho-c-MET and phospho-EGFR could serve as potential biomarkers to identify patients likely to benefit from this combinatorial treatment strategy following development of resistance to PARP inhibitors.

4.3 Future Directions

While our data suggest that the interaction between EGFR and c-MET is likely to contribute to acquired resistance to PARP inhibitors in triple-negative breast cancer. The mechanism underlying this observation remains unknown and should be explored in future studies. Through a systematic search of online databases, we identified 6 proteins known to interact with both EGFR and c-MET that were known to play a role in DNA repair.

FBXO6 is an F box protein that is known to promote replication stress-induced Chk1 degradation. Low levels of FBXO6 has been associated with impairment of Chk1 degradation, leading to replication fork stabilization and activation of DNA repair responses, resulting in resistance to PARP inhibitors through an increased Chk1-mediated DNA damage repair (44).

STUB1 encodes an E3 ubiquitin-protein ligase CHIP which has been shown to ubiquitylate and degrade base excision repair proteins that are not part of the DNA repair complex, resulting in greater efficiency of base excision repair (45) which may in turn lead to resistance to PARP inhibitors.

SFN encodes the protein 14-3-3 sigma which increases non-homologous end joining and upregulates PARP1 expression, enhancing DNA repair (46) and potentially contributing to PARP inhibitor resistance.

CDH1 binds to and activates the anaphase promoting complex or cyclosome (APC/C) which degrades Plk1 in response to DNA damage and prevents cell cycle progression past G2 in cells with DNA damage (47). Additionally, depleting CDH1 impairs Chk1 phosphorylation which may also reduce a cell's ability to repair damaged DNA (47). Thus, since CDH1 contributes maintaining genomic integrity in cells, its activation may limit sensitivity to PARP inhibitors.

TP53 plays a crucial role in maintaining genomic stability (48) and it is plausible that EGFR and/or c-MET may, through its interaction with p53, promote its ability to prevent catastrophic DNA damage, inducing resistance to PARP inhibitors.

PTEN was recently demonstrated to promote repair of double strand DNA breaks via homologous recombination and loss of PTEN improved sensitivity to PARP inhibitors (49). Thus, whether EGFR and/or c-MET promotes PARP inhibitor resistance by enhancing PTEN activity remains an open question.

BIBLIOGRAPHY

1. Yam, C., S. A. Mani, and S. L. Moulder. 2017. Targeting the Molecular Subtypes of Triple Negative Breast Cancer: Understanding the Diversity to Progress the Field. *The oncologist* 22: 1086-1093.
2. Morris, G. J., S. Naidu, A. K. Topham, F. Guiles, Y. Xu, P. McCue, G. F. Schwartz, P. K. Park, A. L. Rosenberg, K. Brill, and E. P. Mitchell. 2007. Differences in breast carcinoma characteristics in newly diagnosed African-American and Caucasian patients: a single-institution compilation compared with the National Cancer Institute's Surveillance, Epidemiology, and End Results database. *Cancer* 110: 876-884.
3. Onitilo, A. A., J. M. Engel, R. T. Greenlee, and B. N. Mukesh. 2009. Breast cancer subtypes based on ER/PR and Her2 expression: comparison of clinicopathologic features and survival. *Clin Med Res* 7: 4-13.
4. Bauer, K. R., M. Brown, R. D. Cress, C. A. Parise, and V. Caggiano. 2007. Descriptive analysis of estrogen receptor (ER)-negative, progesterone receptor (PR)-negative, and HER2-negative invasive breast cancer, the so-called triple-negative phenotype: a population-based study from the California cancer Registry. *Cancer* 109: 1721-1728.
5. Thike, A. A., P. Y. Cheok, A. R. Jara-Lazaro, B. Tan, P. Tan, and P. H. Tan. 2010. Triple-negative breast cancer: clinicopathological characteristics and relationship with basal-like breast cancer. *Mod Pathol* 23: 123-133.
6. Dent, R., M. Trudeau, K. I. Pritchard, W. M. Hanna, H. K. Kahn, C. A. Sawka, L. A. Lickley, E. Rawlinson, P. Sun, and S. A. Narod. 2007. Triple-negative breast cancer: clinical features and patterns of recurrence. *Clin Cancer Res* 13: 4429-4434.

7. Carey, L. A., E. C. Dees, L. Sawyer, L. Gatti, D. T. Moore, F. Collichio, D. W. Ollila, C. I. Sartor, M. L. Graham, and C. M. Perou. 2007. The triple negative paradox: primary tumor chemosensitivity of breast cancer subtypes. *Clin Cancer Res* 13: 2329-2334.
8. Haffty, B. G., Q. Yang, M. Reiss, T. Kearney, S. A. Higgins, J. Weidhaas, L. Harris, W. Hait, and D. Toppmeyer. 2006. Locoregional relapse and distant metastasis in conservatively managed triple negative early-stage breast cancer. *J Clin Oncol* 24: 5652-5657.
9. Symmans, W. F., C. Wei, R. Gould, X. Yu, Y. Zhang, M. Liu, A. Walls, A. Bousamra, M. Ramineni, B. Sinn, K. Hunt, T. A. Buchholz, V. Valero, A. U. Buzdar, W. Yang, A. M. Brewster, S. Moulder, L. Pusztai, C. Hatzis, and G. N. Hortobagyi. 2017. Long-Term Prognostic Risk After Neoadjuvant Chemotherapy Associated With Residual Cancer Burden and Breast Cancer Subtype. *J Clin Oncol* 35: 1049-1060.
10. Peshkin, B. N., M. L. Alabek, and C. Isaacs. 2010. BRCA1/2 mutations and triple negative breast cancers. *Breast Dis* 32: 25-33.
11. Denkert, C., C. Liedtke, A. Tutt, and G. von Minckwitz. 2017. Molecular alterations in triple-negative breast cancer-the road to new treatment strategies. *Lancet* 389: 2430-2442.
12. Belli, C., B. A. Duso, E. Ferraro, and G. Curigliano. 2019. Homologous recombination deficiency in triple negative breast cancer. *Breast* 45: 15-21.
13. Robson, M., S. A. Im, E. Senkus, B. Xu, S. M. Domchek, N. Masuda, S. Delaloge, W. Li, N. Tung, A. Armstrong, W. Wu, C. Goessl, S. Runswick, and P. Conte. 2017.

- Olaparib for Metastatic Breast Cancer in Patients with a Germline BRCA Mutation. *N Engl J Med* 377: 523-533.
14. Litton, J. K., H. S. Rugo, J. Ettl, S. A. Hurvitz, A. Goncalves, K. H. Lee, L. Fehrenbacher, R. Yerushalmi, L. A. Mina, M. Martin, H. Roche, Y. H. Im, R. G. W. Quek, D. Markova, I. C. Tudor, A. L. Hannah, W. Eiermann, and J. L. Blum. 2018. Talazoparib in Patients with Advanced Breast Cancer and a Germline BRCA Mutation. *N Engl J Med* 379: 753-763.
 15. Norquist, B., K. A. Wurz, C. C. Pennil, R. Garcia, J. Gross, W. Sakai, B. Y. Karlan, T. Taniguchi, and E. M. Swisher. 2011. Secondary somatic mutations restoring BRCA1/2 predict chemotherapy resistance in hereditary ovarian carcinomas. *J Clin Oncol* 29: 3008-3015.
 16. Bouwman, P., A. Aly, J. M. Escandell, M. Pieterse, J. Bartkova, H. van der Gulden, S. Hiddingh, M. Thanasoula, A. Kulkarni, Q. Yang, B. G. Haffty, J. Tommiska, C. Blomqvist, R. Drapkin, D. J. Adams, H. Nevanlinna, J. Bartek, M. Tarsounas, S. Ganesan, and J. Jonkers. 2010. 53BP1 loss rescues BRCA1 deficiency and is associated with triple-negative and BRCA-mutated breast cancers. *Nat Struct Mol Biol* 17: 688-695.
 17. Peng, G., C. Chun-Jen Lin, W. Mo, H. Dai, Y. Y. Park, S. M. Kim, Y. Peng, Q. Mo, S. Siwko, R. Hu, J. S. Lee, B. Hennessy, S. Hanash, G. B. Mills, and S. Y. Lin. 2014. Genome-wide transcriptome profiling of homologous recombination DNA repair. *Nat Commun* 5: 3361.
 18. McCann, K. E. 2019. Poly-ADP-ribosyl-polymerase inhibitor resistance mechanisms and their therapeutic implications. *Curr Opin Obstet Gynecol* 31: 12-17.

19. Sugimura, K., S. Takebayashi, H. Taguchi, S. Takeda, and K. Okumura. 2008. PARP-1 ensures regulation of replication fork progression by homologous recombination on damaged DNA. *J Cell Biol* 183: 1203-1212.
20. Ronson, G. E., A. L. Piberger, M. R. Higgs, A. L. Olsen, G. S. Stewart, P. J. McHugh, E. Petermann, and N. D. Lakin. 2018. PARP1 and PARP2 stabilise replication forks at base excision repair intermediates through Fbh1-dependent Rad51 regulation. *Nat Commun* 9: 746.
21. Bhat, K. P., and D. Cortez. 2018. RPA and RAD51: fork reversal, fork protection, and genome stability. *Nat Struct Mol Biol* 25: 446-453.
22. Ray Chaudhuri, A., E. Callen, X. Ding, E. Gogola, A. A. Duarte, J. E. Lee, N. Wong, V. Lafarga, J. A. Calvo, N. J. Panzarino, S. John, A. Day, A. V. Crespo, B. Shen, L. M. Starnes, J. R. de Ruiter, J. A. Daniel, P. A. Konstantinopoulos, D. Cortez, S. B. Cantor, O. Fernandez-Capetillo, K. Ge, J. Jonkers, S. Rottenberg, S. K. Sharan, and A. Nussenzweig. 2016. Replication fork stability confers chemoresistance in BRCA-deficient cells. *Nature* 535: 382-387.
23. Rondinelli, B., E. Gogola, H. Yucel, A. A. Duarte, M. van de Ven, R. van der Sluijs, P. A. Konstantinopoulos, J. Jonkers, R. Ceccaldi, S. Rottenberg, and A. D. D'Andrea. 2017. EZH2 promotes degradation of stalled replication forks by recruiting MUS81 through histone H3 trimethylation. *Nat Cell Biol* 19: 1371-1378.
24. Makvandi, M., A. Pantel, L. Schwartz, E. Schubert, K. Xu, C. J. Hsieh, C. Hou, H. Kim, C. C. Weng, H. Winters, R. Doot, M. D. Farwell, D. A. Pryma, R. A. Greenberg, D. A. Mankoff, F. Simpkins, R. H. Mach, and L. L. Lin. 2018. A PET imaging agent for evaluating PARP-1 expression in ovarian cancer. *J Clin Invest* 128: 2116-2126.

25. Pettitt, S. J., D. B. Krastev, I. Brandsma, A. Drean, F. Song, R. Aleksandrov, M. I. Harrell, M. Menon, R. Brough, J. Campbell, J. Frankum, M. Raney, H. N. Pemberton, R. Rafiq, K. Fenwick, A. Swain, S. Guettler, J. M. Lee, E. M. Swisher, S. Stoyanov, K. Yusa, A. Ashworth, and C. J. Lord. 2018. Genome-wide and high-density CRISPR-Cas9 screens identify point mutations in PARP1 causing PARP inhibitor resistance. *Nat Commun* 9: 1849.
26. Rottenberg, S., J. E. Jaspers, A. Kersbergen, E. van der Burg, A. O. Nygren, S. A. Zander, P. W. Derksen, M. de Bruin, J. Zevenhoven, A. Lau, R. Boulter, A. Cranston, M. J. O'Connor, N. M. Martin, P. Borst, and J. Jonkers. 2008. High sensitivity of BRCA1-deficient mammary tumors to the PARP inhibitor AZD2281 alone and in combination with platinum drugs. *Proc Natl Acad Sci U S A* 105: 17079-17084.
27. Branzei, D., and M. Foiani. 2008. Regulation of DNA repair throughout the cell cycle. *Nat Rev Mol Cell Biol* 9: 297-308.
28. Bajrami, I., J. R. Frankum, A. Konde, R. E. Miller, F. L. Rehman, R. Brough, J. Campbell, D. Sims, R. Rafiq, S. Hooper, L. Chen, I. Kozarewa, I. Assiotis, K. Fenwick, R. Natrajan, C. J. Lord, and A. Ashworth. 2014. Genome-wide profiling of genetic synthetic lethality identifies CDK12 as a novel determinant of PARP1/2 inhibitor sensitivity. *Cancer Res* 74: 287-297.
29. Blazek, D., J. Kohoutek, K. Bartholomeeusen, E. Johansen, P. Hulinkova, Z. Luo, P. Cimermancic, J. Ule, and B. M. Peterlin. 2011. The Cyclin K/Cdk12 complex maintains genomic stability via regulation of expression of DNA damage response genes. *Genes Dev* 25: 2158-2172.

30. Johnson, S. F., C. Cruz, A. K. Greifenberg, S. Dust, D. G. Stover, D. Chi, B. Primack, S. Cao, A. J. Bernhardt, R. Coulson, J. B. Lazaro, B. Kochupurakkal, H. Sun, C. Unitt, L. A. Moreau, K. A. Sarosiek, M. Scaltriti, D. Juric, J. Baselga, A. L. Richardson, S. J. Rodig, A. D. D'Andrea, J. Balmana, N. Johnson, M. Geyer, V. Serra, E. Lim, and G. I. Shapiro. 2016. CDK12 Inhibition Reverses De Novo and Acquired PARP Inhibitor Resistance in BRCA Wild-Type and Mutated Models of Triple-Negative Breast Cancer. *Cell Rep* 17: 2367-2381.
31. Alagpulinsa, D. A., S. Ayyadevara, S. Yaccoby, and R. J. Shmookler Reis. 2016. A Cyclin-Dependent Kinase Inhibitor, Dinaciclib, Impairs Homologous Recombination and Sensitizes Multiple Myeloma Cells to PARP Inhibition. *Mol Cancer Ther* 15: 241-250.
32. Garcia, T. B., J. C. Snedeker, D. Baturin, L. Gardner, S. P. Fosmire, C. Zhou, C. T. Jordan, S. Venkataraman, R. Vibhakar, and C. C. Porter. 2017. A Small-Molecule Inhibitor of WEE1, AZD1775, Synergizes with Olaparib by Impairing Homologous Recombination and Enhancing DNA Damage and Apoptosis in Acute Leukemia. *Mol Cancer Ther* 16: 2058-2068.
33. Tapia-Alveal, C., T. M. Calonge, and M. J. O'Connell. 2009. Regulation of chk1. *Cell Div* 4: 8.
34. Booth, L., J. Roberts, A. Poklepovic, and P. Dent. 2018. The CHK1 inhibitor SRA737 synergizes with PARP1 inhibitors to kill carcinoma cells. *Cancer Biol Ther* 19: 786-796.
35. Du, Y., H. Yamaguchi, Y. Wei, J. L. Hsu, H. L. Wang, Y. H. Hsu, W. C. Lin, W. H. Yu, P. G. Leonard, G. R. t. Lee, M. K. Chen, K. Nakai, M. C. Hsu, C. T. Chen, Y. Sun,

- Y. Wu, W. C. Chang, W. C. Huang, C. L. Liu, Y. C. Chang, C. H. Chen, M. Park, P. Jones, G. N. Hortobagyi, and M. C. Hung. 2016. Blocking c-Met-mediated PARP1 phosphorylation enhances anti-tumor effects of PARP inhibitors. *Nat Med* 22: 194-201.
36. Dong, Q., Y. Du, H. Li, C. Liu, Y. Wei, M. K. Chen, X. Zhao, Y. Y. Chu, Y. Qiu, L. Qin, H. Yamaguchi, and M. C. Hung. 2019. EGFR and c-MET Cooperate to Enhance Resistance to PARP Inhibitors in Hepatocellular Carcinoma. *Cancer Res* 79: 819-829.
37. Linklater, E. S., E. A. Tovar, C. J. Essenburg, L. Turner, Z. Madaj, M. E. Winn, M. K. Melnik, H. Korkaya, C. R. Maroun, J. G. Christensen, M. R. Steensma, J. L. Boerner, and C. R. Graveel. 2016. Targeting MET and EGFR crosstalk signaling in triple-negative breast cancers. *Oncotarget* 7: 69903-69915.
38. Romano, P., A. Manniello, O. Aresu, M. Armento, M. Cesaro, and B. Parodi. 2009. Cell Line Data Base: structure and recent improvements towards molecular authentication of human cell lines. *Nucleic Acids Res* 37: D925-932.
39. Chou, T. C., and P. Talalay. 1984. Quantitative analysis of dose-effect relationships: the combined effects of multiple drugs or enzyme inhibitors. *Adv Enzyme Regul* 22: 27-55.
40. Yam, C. 2017. A Multicenter Phase I Study Evaluating Dual PI3K and BRAF Inhibition with PX-866 and Vemurafenib in Patients with Advanced BRAF V600-Mutant Solid Tumors.
41. Viticchie, G., and P. A. J. Muller. 2015. c-Met and Other Cell Surface Molecules: Interaction, Activation and Functional Consequences. *Biomedicines* 3: 46-70.
42. Symmans, W. F., F. Peintinger, C. Hatzis, R. Rajan, H. Kuerer, V. Valero, L. Assad, A. Poniecka, B. Hennesy, M. Green, A. U. Buzdar, S. E. Singletary, G. N. Hortobagyi,

- and L. Pusztai. 2007. Measurement of residual breast cancer burden to predict survival after neoadjuvant chemotherapy. *J Clin Oncol* 25: 4414-4422.
43. Kim, H. P., Y. K. Yoon, J. W. Kim, S. W. Han, H. S. Hur, J. Park, J. H. Lee, D. Y. Oh, S. A. Im, Y. J. Bang, and T. Y. Kim. 2009. Lapatinib, a dual EGFR and HER2 tyrosine kinase inhibitor, downregulates thymidylate synthase by inhibiting the nuclear translocation of EGFR and HER2. *PLoS One* 4: e5933.
44. Zhang, Y. W., J. Brognard, C. Coughlin, Z. You, M. Dolled-Filhart, A. Aslanian, G. Manning, R. T. Abraham, and T. Hunter. 2009. The F box protein Fbx6 regulates Chk1 stability and cellular sensitivity to replication stress. *Mol Cell* 35: 442-453.
45. Parsons, J. L., P. S. Tait, D. Finch, Dianova, II, S. L. Allinson, and G. L. Dianov. 2008. CHIP-mediated degradation and DNA damage-dependent stabilization regulate base excision repair proteins. *Mol Cell* 29: 477-487.
46. Chen, Y., Z. Li, Z. Dong, J. Beebe, K. Yang, L. Fu, and J. T. Zhang. 2017. 14-3-3sigma Contributes to Radioresistance By Regulating DNA Repair and Cell Cycle via PARP1 and CHK2. *Mol Cancer Res* 15: 418-428.
47. Bassermann, F., D. Frescas, D. Guardavaccaro, L. Busino, A. Peschiaroli, and M. Pagano. 2008. The Cdc14B-Cdh1-Plk1 axis controls the G2 DNA-damage-response checkpoint. *Cell* 134: 256-267.
48. Reinhardt, H. C., and B. Schumacher. 2012. The p53 network: cellular and systemic DNA damage responses in aging and cancer. *Trends Genet* 28: 128-136.
49. Mansour, W. Y., P. Tennstedt, J. Volquardsen, C. Oing, M. Kluth, C. Hube-Magg, K. Borgmann, R. Simon, C. Petersen, E. Dikomey, and K. Rothkamm. 2018. Loss of PTEN-assisted G2/M checkpoint impedes homologous recombination repair and

enhances radio-curability and PARP inhibitor treatment response in prostate cancer.

Sci Rep 8: 3947.

VITA

Clinton Yam was born in Singapore. He graduated with a Bachelor's Degree in Medicine and Surgery (MBBS) with Honors from the National University of Singapore in 2008. He worked as a research assistant at the University of California, San Diego for a year following his graduation before returning to Singapore for his internship and residency in internal medicine. He then served as a medical officer in the Republic of Singapore Navy for 2 years before returning to the United States for his internal medicine residency at the University of Pennsylvania. After completing his residency, he moved to Houston, TX for his medical oncology and hematology fellowship at The University of Texas MD Anderson Cancer Center. In August 2017, he enrolled in the Masters of Science Program in The University of Texas MD Anderson Cancer Center UTHHealth Graduate School of Biomedical Sciences.